



**HAL**  
open science

## Measuring techniques in gas–liquid and gas–liquid–solid reactors

Cristophe Boyer, Anne-Marie Duquenne, Gabriel Wild

► **To cite this version:**

Cristophe Boyer, Anne-Marie Duquenne, Gabriel Wild. Measuring techniques in gas–liquid and gas–liquid–solid reactors. *Chemical Engineering Science*, 2002, vol. 57 (n° 16), pp. 3185-3215. 10.1016/S0009-2509(02)00193-8 . hal-01394969

**HAL Id: hal-01394969**

**<https://hal.science/hal-01394969>**

Submitted on 10 Nov 2016

**HAL** is a multi-disciplinary open access archive for the deposit and dissemination of scientific research documents, whether they are published or not. The documents may come from teaching and research institutions in France or abroad, or from public or private research centers.

L'archive ouverte pluridisciplinaire **HAL**, est destinée au dépôt et à la diffusion de documents scientifiques de niveau recherche, publiés ou non, émanant des établissements d'enseignement et de recherche français ou étrangers, des laboratoires publics ou privés.



## Open Archive TOULOUSE Archive Ouverte (OATAO)

OATAO is an open access repository that collects the work of Toulouse researchers and makes it freely available over the web where possible.

This is an author-deposited version published in : <http://oatao.univ-toulouse.fr/>  
Eprints ID : 16521

**To link to this article** : DOI : 10.1016/S0009-2509(02)00193-8  
URL : [http://dx.doi.org/10.1016/S0009-2509\(02\)00193-8](http://dx.doi.org/10.1016/S0009-2509(02)00193-8)

<p><b>To cite this version</b> : Boyer, Christophe and Billet, Anne-Marie and Wild, Gabriel <i>Measuring techniques in gas-liquid and gas-liquid-solid reactors</i>. (2002) <i>Chemical Engineering Science</i>, vol. 57 (n° 16). pp. 3185-3215. ISSN 0009-2509</p>
---

Any correspondence concerning this service should be sent to the repository administrator: [staff-oatao@listes-diff.inp-toulouse.fr](mailto:staff-oatao@listes-diff.inp-toulouse.fr)

# Measuring techniques in gas–liquid and gas–liquid–solid reactors

Christophe Boyer<sup>a,\*</sup>, Anne-Marie Duquenne<sup>b</sup>, Gabriel Wild<sup>c</sup>

<sup>a</sup>Centre d'études et de développement industriels (CEDI) "René Navarre" BP no 3, F 69390, Vernaison France

<sup>b</sup>Laboratoire de Génie Chimique, ENSIACET—CNRS (UMR no 5503) 18 chemin de la Loge, F 31078 Toulouse cedex 04, France

<sup>c</sup>Laboratoire des Sciences du Génie Chimique, CNRS (UPR no 6811)—ENSIC, B.P. 451, F 54001 Nancy, France

## Abstract

This article offers an overview of the instrumentation techniques developed for multiphase flow analysis either in gas/liquid or in gas/liquid/solid reactors. To characterise properly such reactors, experimental data have to be acquired at different space scale or time frequency. The existing multiphase flow metering techniques described give information concerning reactor hydrodynamics such as pressure, phases holdups, phases velocities, flow regime, size and shape of dispersed inclusions, axial diffusion coefficients. The measuring techniques are presented in two groups: the non-intrusive techniques that deliver global, cross-section-averaged or local data, and the intrusive probes that are dedicated to local measurements. Eventually some examples of multiphase instrumentation development are reported (trickle-bed and slurry bubble column at semi-industrial scale) in the refinery or petrochemical area.

© 2002 Elsevier Science Ltd. All rights reserved.

## 1. Introduction

The description and design of gas–liquid and gas–liquid–solid reactors still relies to a large extent on empirical rules and correlations, which in turn are based on measurements made under conditions as relevant as possible to industrial practice. This is true for the classical chemical engineering approach, where such quantities as liquid holdup or pressure drop are predicted via empirical correlations based on data as numerous and precise as possible. Nevertheless, more modern approaches such as computational fluid dynamic (CFD) are used to help in the design of multiphase reactors. Even in this case, the physical models used require information on local and transient flow characteristics (e.g. turbulence characteristics, wake coefficients, etc.), since ab initio calculations are up to now impossible.

Reliable measuring techniques are therefore needed as well in academia as in industry for the rational description and the design of multiphase reactors. Depending on the aim of the analysis, different types of measurements are required and it is important to maintain an adequacy of space and

time resolution of the technique used and the purpose of the study.

Measurement techniques can be classified according different ways. A first classification distinguishes between time-averaged and transient measurements and between local and global measurements. According to this classification, the following types of values or characteristics are measured:

- Global steady-state characteristics of the reactor (gas or liquid holdup, pressure drop, flow regime, minimum fluidisation velocity, etc.)
- "Local" time-averaged characteristics
- One-dimensional space: cross-section-averaged values at a given level of a reactor
- Two-dimensional space: local averaged values over a reactor cross-section (tomographic techniques)
- Three-dimensional space
- Local and transient characteristics of the flow field.

The local and/or transient character of the measurement can vary widely, depending on the time and the length scale.

As an example, in case of the design of a trickle bed reactor, liquid distribution is of the utmost importance, but in most cases the flow is fairly steady state. In this case, for

\* Corresponding author.

E-mail addresses: [christophe.boyer@ifp.fr](mailto:christophe.boyer@ifp.fr) (C. Boyer),  
[annemarie.duquenne@ensigct.fr](mailto:annemarie.duquenne@ensigct.fr) (A.-M. Duquenne),  
[gabriel.wild@ensic.inpl-nancy.fr](mailto:gabriel.wild@ensic.inpl-nancy.fr) (G. Wild).

local time averaged, at least 2D measuring techniques of the liquid velocity or liquid holdup are needed. In case of a slurry bubble column, global characteristics are required (minimum settling velocity) but also local ones, like the local liquid velocity and gas and solid holdup. These measurement needs will be illustrated at the end of this paper by presenting some examples of instrumentation development in the oil industry.

Since the classification between local and global measurement is not always possible another classification has been preferred in this article. This classification relies more on the physical basis of the measurement and finally one can distinguish between invasive and non-invasive measuring techniques.

In the present work, a review of a number of non-invasive and invasive measuring techniques is presented. In both cases (non-invasive and invasive) the techniques are grouped according to the physical principle of the measurement. In the meantime, the characteristics of the techniques according to the first classification (global or local, time averaged or transient) are indicated as well as orders of magnitude of the length and time resolution to be expected. Finally, some examples of the use of measuring techniques with industrial constraint in the petrochemical and refinery industry are presented.

## 2. Non-invasive techniques

There are numerous non-invasive techniques (Table 1) available to investigate hydrodynamics of gas–liquid and gas–liquid–solid reactors. First, techniques yielding characteristics of the whole reactor or of a part of the reactor (global techniques) will be examined, the characteristics being e.g. the pressure drop, the gas and/or liquid holdup, the flow regime, the bubble size distribution, the mixing characteristics of the gas, the liquid or the solid phase. In some, long-term averages are measured, in others fluctuations are analysed. Next, determination techniques of local characteristics will be presented (gas and liquid velocity, bubble or particle size and position). Often, one single technique can yield more than one characteristic.

### 2.1. Global techniques

#### 2.1.1. Time-averaged pressure drop

The pressure drop between two levels of a reactor is a very important variable to know, either because the *pressure drop* is important per se (design of the pumps and compressors), or because it gives information on the *holdup of the different phases* or on the *flow regime*.

(a) *Measuring technique*. It is recommended to measure the pressure with sensors flush to the wall; the price of piezoelectric pressure sensors decreased in the last 10 years and such equipment is now quite standard. Care must however be taken that no fixed bed solid is directly in contact with the

membrane of the sensor. The interpretation of the pressure drop in terms of static pressure drop and friction pressure drop is not always easy: e.g. in case of trickle beds, the pressure drop measured may be the friction pressure drop or the total pressure drop, depending on the measuring procedure. The large scatter observed in pressure drop data in trickle beds is partly due to the fact that, quite often, the values reported are “somewhere in-between” the friction and the total pressure drop. In bubble columns, slurry bubble columns and three-phase fluidised beds the friction pressure drop is usually negligible compared with the static pressure drop.

$$\frac{\Delta P}{Z} = g(\rho_L \varepsilon_L + \rho_S \varepsilon_S + \rho_G \varepsilon_G) + \left(\frac{\Delta P}{Z}\right) f.$$

(b) *Uses of the mean pressure drop*. The main use of pressure measurements in such pieces of equipment is to *determine gas, liquid and/or solid holdup* (Joshi, Patil, Ranade, & Shah, 1990; Wild & Poncin, 1996) in such reactors. In case of three-phase reactors, the pressure drop measurement has to be combined with another technique to get all the phase holdups.

In multiphase reactors, an exact description of the flow behaviour by CFD is usually still impossible and the design of these reactors usually relies on empirical correlations of a number of characteristics of hydrodynamics, heat and mass transfer. Usually such correlations are valid at the best for a given *flow regime*; defining ways to determine which is the flow regime is therefore an important task. According to Zahradník et al. (1997), three main flow regimes can be distinguished in bubble columns: homogeneous flow, transition flow and established heterogeneous flow; in case of small diameter columns, plug flow must be added. In gas–liquid–solid fluidisation, usually homogeneous flow and heterogeneous flow regime are considered. In trickle beds it is usual to distinguish trickling flow regime (low interaction) and different forms of high-interaction flow regimes (pulsing flow, bubble flow, spray flow, foamy flow, etc.) (Saroha & Nigam, 1996). Time-averaged values of the pressure drop or the phase holdups can be used to determine flow regime transitions but give very uncertain results. This technique has however been used in trickle beds (Purwasasmita, 1985). The classic drift flux analysis of Wallis (1969) (bubble columns) and of Züber and Findlay (1965) (airlift reactors) are relatively easy to use and give fair precision for both flow regime transitions in these reactors (see e.g. Vial et al., 2000).

#### 2.1.2. Measurement and analysis of signal fluctuations

Analysing the fluctuations of a signal depending on the hydrodynamics is a relatively direct way of determining the flow regime in a multiphase reactor. This signal may be a wall pressure (Matsui, 1984; Glasgow, Erickson, Lee, & Patel, 1984; Drahos & Cermak, 1989; Drahos, Zahradník, Puncchar, Fialova, & Bradka, 1991; Drahos, Bradka, & Puncchar, 1992; Vial et al., 2000; Johnsson, Zijerveld, Schouten, van den Bleek, & Leckner, 2000; Kluytmans,

Table 1  
Non-invasive techniques

Technique	Application	Expected results	Limitations	Spatial resolution	Time resolution
Pressure drop	GL and GLS	Pressure drop, liquid holdup, flow regime	Model required Model required	1D	+
Pressure fluctuation	GL and GLS	Flow regime, turbulence characteristics		—	++
Dynamic gas disengagement technique	GL and GLS	Bubble size distribution phase holdup	Model required In case of a slurry	Global technique	Steady state
Tracers	GL and GLS	Liquid holdup and mixing characteristics	Eventually sophisticated model required, finding an adequate tracer	Global technique	Hydrodynamic steady state
Conductimetry	GL and GLS	Liquid holdup	Only electrically conductive liquid, calibration required	1D	+
Neutron absorption $\gamma$ -ray absorption X-ray absorption	GL and GLS	Phase distribution	Neutron source required, safety and price, safety and price	Path averaged values	— —
Light attenuation	GL	Gas holdup and interfacial area	Transparent and clean liquid and wall required, Model required, low holdup and small diameter column	Global	+
Ultrasound attenuation	GL GLS with restrictions	Holdup	Liquid continuous phase, small diameter column	Path averaged values	+
Photography and image analysis	Mainly GL	Bubble/drop size shape Flow regime	Mainly wall region, transparent wall and liquid Low holdup of dispersed phase, quantitative image analysis not always available	++	+
Radiography	Mainly GL	Bubble/drop size and shape, flow regime	Safety, Low gas holdup	++	-+
PIV	Mainly GL (+ seeding)	Gas and liquid velocity fields	Low gas holdup	++	+(no velocity fluctuations observed)
NMR	GL and GLS	Liquid holdup, phases velocity, wetting efficiency	Price and size of equipment	++	+
Laser Doppler Anemometry and phase Doppler anemometry	GL	Mainly liquid velocity, eventually gas velocity and bubble size	Transparent liquid, relatively low holdup, very low holdup, for PDA	+++	++
Polarography (microelectrodes)	GL and GLS	Wall shear stress	Support electrolyte needed, only aqueous solutions	+++	++
Tracking of radioactive particles	GL and GLS	Velocity fields and trajectories	Heavy calibration required, use of radioactive particles	+	+
$\gamma$ - or X-ray tomography	GL and GLS	Phase holdup distribution	Price, high power required for large solid holdup	+	—
Capacitive or resistive tomography	GL and GLS	Phase holdup distribution	No reliable reconstruction algorithm available	—	+++
Ultrasonic tomography	GL and GLS	Phase holdup distribution	Low solid and gas holdup	+—	+

Spatial resolution: +++ :  $\ll$  1 mm; ++  $\sim$  mm; + : cm. Time resolution: +++ : ms; ++ : s; + : minute.

van Wachem, Kuster, & Schouten, 2001), the current at micro-electrodes imbedded in the wall (Latifi, Rode, Midoux, & Storck, 1992; Latifi, Naderifar, & Midoux, 1994a; Latifi, Naderifar, Midoux, & Le Méhauté, 1994b) or in particles (Lesage, 2000) of a trickle bed, conductivity probes (Briens, Briens, Margaritis, & Hay, 1997b; Briens, Briens, Hay, Hudson, & Margaritis, 1997a; Maucci, Briens, Martinuzzi, & Wild, 1999), the sound produced by the flow in a trickle bed (Kolb, Melli, de Santos, & Scriven, 1990), in an airlift reactor (Glasgow, Hua, Yiin, & Erickson, 1992) or in an aerated stirred tank (Boyd & Varley, 1998). Local probe signal from optical probes (e.g. Bakshi, Zhong, Jiang, & Fan, 1995), optical transmittance probes (Kikuchi, Tsutsumi, & Yoshida, 1997), temperature probes (Thimmapuram, Rao, & Saxena, 1992), hot film anemometry (e.g. Magaud, 1999), electrochemical probes (Vial, 2000) can give information of flow regime. Of course, one has to be careful not to over-interpret fluctuations: each measuring technique has an inertia and therefore a time resolution limit. On the other hand with a very fast technique, sampling can be a non-trivial problem, specially with invasive probes, where bubble-probe interactions may prove a problem (see Section 3).

A number of authors have proposed numerical techniques devoted to the interpretation of fluctuations in terms of flow regimes: the possibilities are numerous and range from quite classical techniques like statistical (e.g. Drahos et al., 1991; Letzel, Schouten, Krishna, & van den Bleek, 1997) or spectral (e.g. Bigot, Guyot, Bataille, & Roustan, 1990; Latifi et al., 1992) analysis to modern techniques with a much more sophisticated mathematical background. Such new techniques include fractal analysis (Drahos et al., 1992; Briens et al., 1997b; Maucci et al., 1999; Latifi et al., 1994b; Naderifar, 1995; Luewisuthichat, Tsutsumi, & Yoshida, 1995), chaotic analysis (Luewisuthichat, Tsutsumi, & Yoshida, 1996; Letzel et al., 1997; Johnsson et al., 2000; Lin, Juang, Chen, & Chen, 2001; Kluytmans et al., 2001), time-frequency analysis (Bakshi et al., 1995; Vial et al., 2000). A review on these techniques applied to bubble columns was published recently by Vial et al. (2000).

### 2.1.3. Dynamic gas disengagement technique (DGD)

The basic principle of this technique is to stop the aeration in a gas-liquid or gas-slurry bubble column and to measure the liquid level or the pressure at different levels in the reactor as a function of time. This technique can be used either to determine the *global gas and solid holdup* in a slurry bubble column (see example in Section 4.2), or to determine the *structure of the gas holdup* in bubble columns (amount of gas bubbles separated in classes according to their size). The latter application has been used for some time (Beinhauer, 1971; cited by Deckwer, 1985). The decrease of the liquid level is observed, using various techniques: X-ray (Beinhauer, 1971), visual observation, pressure profile (Daly, Patel, & Bukur, 1992). The basic

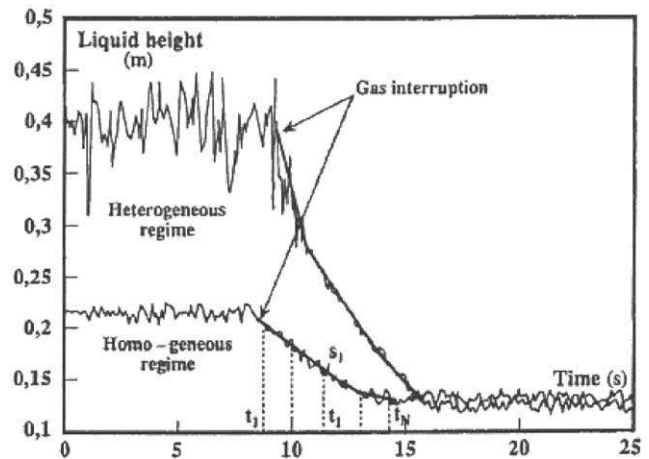


Fig. 1. DGD in a bubble column (Camarasa et al., 1999).

assumptions made in this technique are the following (Camarasa et al., 1999):

- the dispersion is axially homogeneous when the gas feed is interrupted,
- there are no bubble-bubble coalescence or break-up happening during disengagement,
- the bubble disengagement of each bubble class is not influenced by the other bubble classes.

Fig. 1 gives an example of a DGD curve; the liquid height in a bubble column with the system air-water is represented as a function of time (Camarasa et al., 1999). In principle, it is possible to represent this curve by a number of straight lines corresponding each to a bubble class with a given bubble rise velocity. However in practice, a bimodal bubble diameter distribution is usually assumed.

In recent work, Lee, Luo and Fan (1999) checked experimentally the assumptions of DGD in a two-dimensional bubble column by PIV measurements. They show that the assumptions (b) and (c) of the classical DGD technique are not valid, specially in the coalesced bubble flow (heterogeneous or transition) regime. The limits of the application of the DGD technique indicated by these authors have still to be checked in case of three-dimensional columns.

### 2.1.4. Tracing techniques

Tracing techniques are used with two aims:

- determining the mean phase holdup of one of the phases,
- characterising mixing of a phase.

**2.1.4.1. Tracing of the liquid.** Measuring the residence time distribution (RTD) of a tracer of the liquid phase is a well-known technique to determine the mean liquid holdup of a reactor and to characterise the mixing of the liquid phase. However, using this technique presents some pitfalls which shall be presented in the following.

The theory of RTD is well known (Levenspiel, 1999; Villiermaux, 1995; Shah, Stiegel, & Sharma, 1978; Buffham & Mason, 1993). The tracer is in most cases a salt tracer and the measuring technique is conductivity; coloured tracers have also been used, mainly with non-aqueous liquids (see e.g. Lara Márquez, 1992). Radioactive isotope tracer techniques present the advantage that non-invasive measurements are possible at different levels of the reactor (Blet, Berne, Chaussy, Perrin, & Schweich, 1999; Pant, Saroha, & Nigam, 2000). An interesting, if expensive, technique has been proposed recently by Sakai et al. (2000): these authors use a non-radioactive tracer which interacts with neutrons. The advantage is that this technique can be used under high temperature and pressure conditions (coal liquefaction plant in the present case). Of course, a neutron source is required. In Section 4.2 of this paper a refractometry technique is described: in this case the tracer is a liquid whose refractive index is different from that of the main liquid.

In the interpretation of a RTD curve, the actual flow behaviour is represented by a model, with parameters that are adjusted to fit experimental values of the tracer concentration along time. Depending on the complication of the flow behaviour, quite simple models with a limited number of parameters may be used or much more sophisticated ones.

In simple cases, a two-parameter model may be sufficient to yield an adequate description of the global flow behaviour of a reactor: one of these parameters is usually the mean residence time of the liquid (or the linear velocity, or the liquid holdup), the other one being a characteristic of mixing (axial dispersion coefficient, number of CSTRs, recirculation rate between stirred cells). If the RTD has been correctly performed, this yields a quite precise determination of the global liquid holdup. Examples of the application of this technique to the determination of the liquid holdup may be found in Larachi, Laurent, Wild, and Midoux, 1991 (gas-liquid cocurrent flow through a fixed bed of non-porous particles) or in García Ochoa, Khalifet, Poncin, & Wild (1997) (suspended solid bubble column).

In more complex cases, models with more parameters have to be used: e.g. in case of mass transfer between the flowing liquid and stagnant zones, a piston with exchange (PE) or a piston with dispersion and exchange (PDE) may be used as shown e.g. by Yang, Euzen, and Wild (1990) who used the model developed by Villiermaux and van Swaaij (1969) in the case of liquid flow through a bed packed with porous particles. Such models contain more adjustable parameters and care must be taken to check the sensitivity of the agreement between model and experiment with respect to the different parameters. In case of even more complex reactors, with different geometric parts, interpretation of RTD curves becomes even more tricky. In this case, it is advisable to split the reactor up in elementary elements (stirred tanks, plug flow parts, plug flow with axial dispersion, etc.). The volume of each element, the flow rate, etc. should as far as possible be estimated independently of the RTD interpretation to avoid the danger of overfitting. An example of this

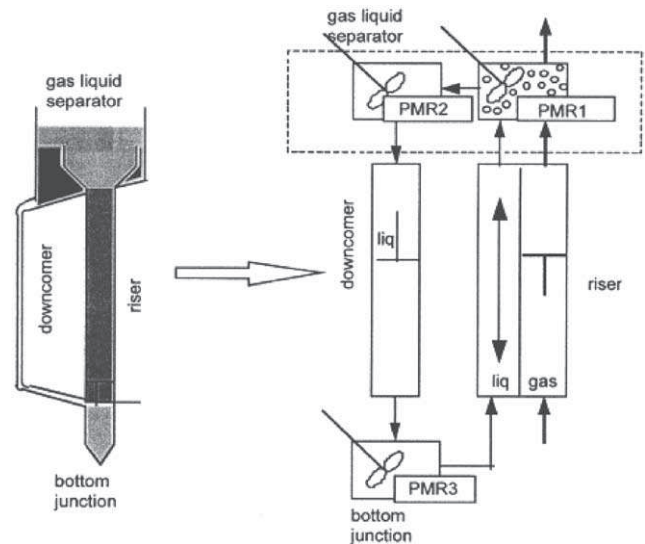


Fig. 2. Model of an airlift reactor (Dhaouadi et al., 1997).

way to proceed is given by Dhaouadi et al. (1997) (Fig. 2): an external loop air-lift reactor is considered as consisting in:

- a single-phase liquid plug flow in the downcomer,
- a single-phase liquid CSTR at the bottom junction,
- a liquid-phase plug flow with axial dispersion flowing cocurrently with gas in the riser,
- a gas-liquid CSTR and a single liquid-phase CSTR in series at the gas-liquid separator.

The volumes of the different parts are estimated independently and the gas holdup in the two gas-liquid parts are determined by pressure measurements, so that the only remaining adjustable parameters are the liquid velocity and the axial dispersion coefficient in the riser. The tracer mass balances in the different parts of the airlift yield a system of ODEs and PDEs which has been solved by using the “MODEST” software package (Haario, 1994) which is dedicated to this kind of problem. Fig. 3 (Dhaouadi et al., 1997) gives an illustration of the quality of the fit obtained in this case.

Under the same considerations, Leclerc, Claudel, Lintz, Potier, and Antoine (2000) presented a software package, the aim of which is to interpret in the best possible way RTD curves in complex systems.

One must keep in mind that the concentrations to be taken into account for RTD analysis are mixing cup concentrations at the inlet, the outlet and eventually at different levels of the reactor. Unfortunately, most measurement techniques determine volume or column diameter averaged concentrations (“through the wall concentrations”) and not mixing cup concentrations. As shown by Briens, Margaritis, and Wild (1995), this can lead to quite important errors in the determination of liquid holdup or liquid residence time, when the flow behaviour is far from plug flow.

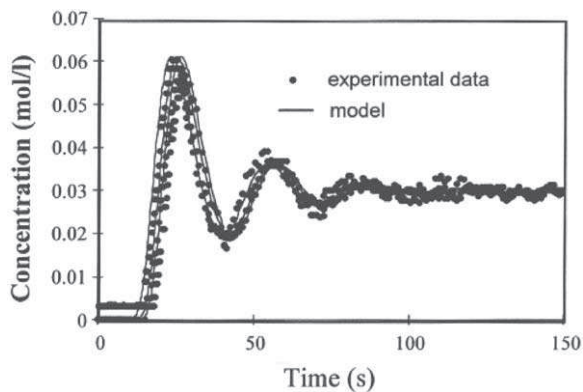


Fig. 3. RTD curves in an airlift reactor compared with an adjusted model (Dhaouadi et al., 1997) (measurements at three levels of the downcomer).

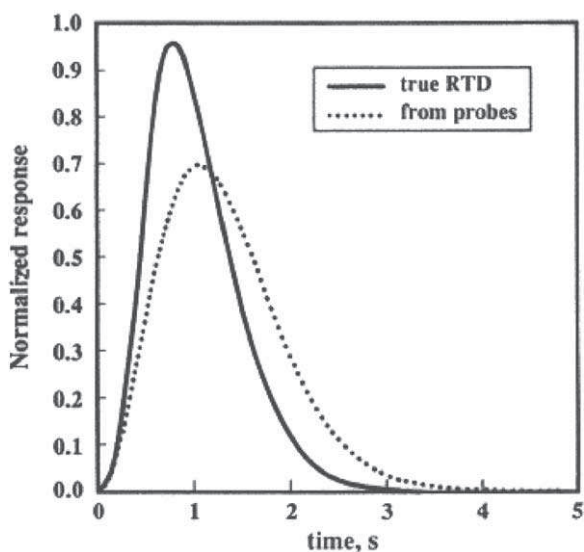


Fig. 4. Comparison of a “through the wall” concentration with the “true” RTD in case of a high level of interaction between fluid elements (Briens et al., 1995).

Fig. 4 shows an example proposed by these authors of the difference between the real RTD curve and a concentration profile as measured by a “through the wall” technique (e.g. a radioactive tracer concentration measurement) in case of a non-ideal flow, with a high level of interaction between fluid elements (Briens et al., 1995). Through the wall techniques can, however, be used to measure the “mixing time” of the liquid. Another point has to be checked: in a number of techniques, the measurement of the liquid-phase concentration is disturbed by the presence of bubbles and the actual signal has to be filtered: this may not be trivial as exemplified by a recent paper of Gupta, Al-Dahhan, Dudukovic, and Mills (2000).

Instead of using a dissolved liquid-phase tracer, it may be of interest to use a particle tracking technique, i.e. a neutrally buoyant solid particle is followed by electromagnetic means

or by the radiation it emits. A review on such techniques may be found in Lübbert (1991); the CARPT (Dudukovic, Devanathan, & Holub, 1991) or RPT (Larachi, Chaouki, & Kennedy, 1995; Chaouki, Larachi, & Dudukovic, 1997) techniques which, will be discussed later, are based on the use of such flow followers, the application of which is restricted to bubble column like reactors.

**2.1.4.2. Tracing of the gas-phase.** Investigation of gas-phase dispersion is more difficult than that of liquid: while there are a number of liquid-phase tracers which can be considered completely non-volatile, there are no completely insoluble gases. Even with the less soluble gases (e.g. Helium in water), absorption and desorption phenomena make the interpretation of gas-phase tracing experiments intricate, as shown by Joseph and Shah (1986). It is therefore necessary to consider simultaneously gas-liquid mass transfer and gas and liquid dispersion. The mixing of the liquid phase may be investigated also, as shown by Mawlana, Huang, Wilhelm, and Delmas (1992). It is however preferable to determine liquid-phase characteristics independently by liquid tracer experiments.

An interesting tracing technique of the gas proposed by Lübbert (1991) relies on a stochastic distribution of the tracer gas with a cross-correlation technique of the outlet signal with the inlet signal.

**2.1.4.3. Tracing of the solid.** Tracing of the solid phase has its importance in fluidisation and there are a number of papers devoted to this subject in gas-solid fluidisation. In gas-liquid-solid and liquid-solid fluidisation, it is of the utmost importance that the shape, size and density of the tracer particles be the same as those of the fluidised particles. Three kinds of tracers have been used:

- Coloured tracers: investigating the behaviour of layers of particles of different colours gives mainly qualitative information on the mixing of the solid. Furthermore, separating the particles according to the colours can prove tiresome. Nevertheless, this technique has been used by Fortin (1984).
- Magnetic tracers: Euzen and Fortin (1987); see also Wild and Poncin (1996) proposed to impregnate porous catalyst particles with a ferromagnetic substance (e.g. Nickel oxide which is reduced to Nickel). Two concentric loops are situated around the column. The signal measured in the inner loop in presence of an electric current (in the outer loop) depends on the magnetic properties in the column at the level of the loop. Furthermore, the magnetic properties of the tracer particles can be used to separate them from the inert particles and so use them again. A similar technique had been used in liquid-solid fluidisation in the sixties (Flaschel, Metzdorf, & Renken, 1987).
- Fluorescent tracers: in case of liquid-solid slurries, Flaschel et al. (1987) proposed to use as a tracer solid particles on which a fluorescing substance was adsorbed.

This technique should be applicable also in three-phase systems.

#### 2.1.5. Conductimetry

If the liquid in a gas–liquid or gas–liquid–solid reactor is electrically conductive and presents a constant ionic concentration, the conductivity between two levels of the reactor is an increasing function of the liquid holdup. Unfortunately, the conductivity depends not only on the liquid holdup, but also on the spatial distribution of the phases. A number of mainly empirical “laws” have been proposed to correlate the liquid saturation  $\beta_L$  (i.e. the ratio of the liquid holdup to the liquid holdup in absence of gas) with the conductivity in presence and in absence of gas (Storck, Latifi, Barthole, Laurent, & Charpentier 1986), which can give quite different results (as much as 20% difference between the predictions of  $\beta_L$ ). It is therefore advisable to calibrate this technique by another one.

This technique has however been used in a number of fields: Begovich and Watson (1978) investigated the behaviour of three-phase fluidised beds, Uribe-Salas, Gomez, and Finch (1994) and Shen and Finch (1996) used it in bubble columns.

An elegant variation of the conductimetric technique was proposed by Shen and Finch (1996) to determine bubble swarm velocity in a bubble column. These authors developed a fast conductimetre; the bubbles disturb the conductimetry signal and the propagation celerity of this perturbation can be interpreted as a measure of the bubble swarm velocity. Note that in this case it is no longer necessary to know the quantitative correlation of the liquid holdup as a function of the conductivity.

#### 2.1.6. Radiation attenuation techniques

When crossing a two-phase mixture, all kinds of radiation are attenuated. Depending on the kind of radiation used, the attenuation is function of the density along the radiation path or of the interfacial area.

(a) *X-ray,  $\gamma$ -ray or neutron absorption radiography.* Gases, liquids and solids have quite different absorption coefficients of X-ray or  $\gamma$ -ray radiation or of neutron beams. The measurement of the attenuation of such a radiation between a source and a receptor on the other side of the reactor gives access to the integral of the local mass density distribution along the path of the beam. The basics and the limits of the radiography techniques using this principle may be found in Fournier and Jeandey (1993). There are no theoretical limits to time resolution; limits are, however, given by safety and/or price considerations. Space resolution is limited by the size of the available sensors ( $\sim 10$  mm in case of  $\gamma$ -rays, 100  $\mu$ m in case of X rays). These radiographic techniques are the basis of a number of tomographic techniques (see Section 4.1).

(b) *Light attenuation.* In case of a clean transparent liquid containing bubbles or drops, the light attenuation is an

increasing function of the specific interfacial area of the dispersed phase. The first applications of this technique were limited to quite small interfacial areas and required that no multiple scattering of the light beam by the bubbles take place (Calderbank, 1958) and the optical density  $aL$  (i.e. the product  $aL$ ,  $a$  being the interfacial area per volume and  $L$  the optical path length) was limited to quite small values. Work done since this period (Kasireddy & Al Taweel, 1990) has extended the possible values of  $aL$  up to much higher values ( $aL_{\max} = 2500$ ). However, the bubbles have to be approximately spherical and stringent measures have to be taken to avoid parasitic light sources, electronic noise, liquid turbidity, etc.

(c) *Ultrasound techniques.* The main advantage of ultrasound-based measurement techniques, compared to visible radiation based techniques, is that transparency of the liquid is not required. Some of the ultrasound techniques being invasive, ultrasound techniques will therefore be treated in Section 3.3

## 2.2. Techniques yielding local characteristics

### 2.2.1. Visualisation techniques

Visualisation techniques yield bubble shape and size. They can be classified into photographic (including of course video) techniques and radiographic techniques, Particle Image Velocimetry and techniques based on NMR.

(a) *Photographic techniques.* The aspect of the flow as seen through the wall is an important feature, and taking pictures through the wall is very frequent in literature (e.g. Miyahara, Hamaguchi, Sukeda, & Takahashi, 1986; Lage & Espósito, 1999). The limitations of this technique are obvious: only the vicinity of the wall can be observed at high gassing rates; a transparent wall, a transparent liquid are required. In case of high pressure columns, visualisation requires special windows: Lin, Tsuchiya, and Fan (1998) use quartz windows that can stand pressures up to 20 MPa.

The bubbles in most kinds of equipment are not spherical and can vary widely in shape. Quantitative image analysis can allow to determine, beside the area mean diameter such quantities as the Fétet diameters, the sphericity, etc. (Bendjaballah et al., 1999; Camarasa et al., 1999). In three-phase systems, refractive index matching of the solid and the liquid can allow to determine bubble size and shape. This technique was used by Peterson, Tankin, and Bankoff (1984) to investigate three-phase fluidised beds. It is however quite cumbersome and seldom used.

(b) *Radiographic techniques.* Using more energetic kinds of radiation to observe bubble forms is an extension of the photographic technique: e.g. Heindel (2000) uses the Flash X-ray Radiography to determine the evolution of bubble shape and position. The advantage is that such a technique may yield results even in presence of a non-transparent fluid; as with the photographic technique, only a single layer of

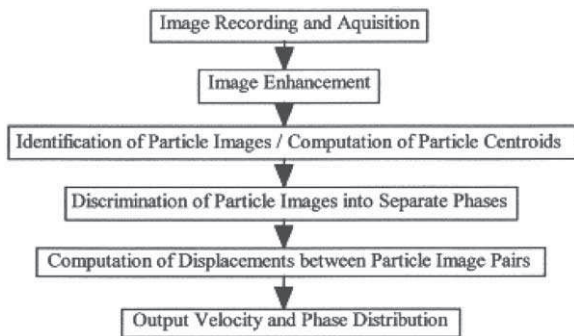


Fig. 5. Flow sheet of the PIV system with a particle tracking algorithm (Reese et al., 1996).

bubbles can be observed reliably. A similar technique has been used by Smith, Gamblin, and Newton (1995).

2D or 3D images of the multiphase flow can be obtained using tomographic techniques (based on radiography), either time averaged or instantaneous. These techniques will be considered separately in this article (see Section 2.2.4).

(c) *Particle image velocimetry*. This technique has become quite classical for the determination of velocity fields in single-phase flow. A laser sheet is used to illuminate a well defined slice of the fluid containing seeding particles; two or more pictures of the sheet are taken at short time intervals. The distances between the positions of seeding particles yield the instantaneous velocity field of the liquid. Different variants have been proposed: particle streak velocimetry (long exposure), particle tracking velocimetry (video recording of particle motion).

In recent years, a number of authors have used PIV in gas-liquid flow to determine either the liquid velocity field or the bubble velocity and size, or both. Reviews on this subject may be found in Murai et al. (2000); Chaouki et al. (1997) or Reese, Mudde, Lee, and Fan (1996). The main problem is to identify the particles between the different frames. Fig. 5 shows a flow chart of a two-phase PIV system, as proposed by Reese et al. (1996). In order to discriminate the different phases, a number of possibilities have been proposed: using fluorescent seeding particles for the liquid and filtering the signals (e.g. Bröder, Lain, & Sommerfeld, 2000). The same technique combined with refractive index matching has been used by Northrup, Kulp, Angel, and Pinder (1993) to determine interstitial velocity fields in a fixed bed. It is also possible to use numerical techniques to exploit images obtained with a single CDD camera as shown by Delnoij, Kuipers, van Swaaij, and Westerweel (2000); the latter authors propose an original “Ensemble correlation” technique to extract the relevant signals from the results obtained with a CDD camera. Recently, PIV has been applied to confirm the predictions of velocity calculations in visco-elastic liquids around rising bubbles (Funfschilling & Li, 2001).

(d) *NMR imaging*. Nuclear magnetic resonance (NMR) imaging has been widely used in the field of medical imaging and is more and more frequently applied to chemical engineering problems. The theoretical background of these tech-

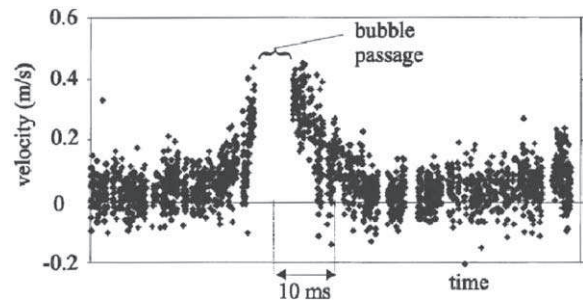


Fig. 6. LDA velocity signal in a bubbly system (Müdde, Groen, & van den Akker, 1998).

niques may be found in Callaghan (1991). It is based on the determination voxel by voxel of the quantity of given nuclei (usually protons  $^1\text{H}$ ); radio-frequency pulses and magnetic field gradient pulses interact with the spins of the nuclei positioned in a static magnetic field. Reviews on the application in the fields of chemical engineering are proposed by Gladden (1994) or Chaouki et al. (1997). In the last years, some applications of this still quite expensive technique in the investigation of fixed bed reactors have been found in literature (Sederman, Johns, Bramley, Alexander, & Gladden, 1997; Sederman, Johns, Alexander, & Gladden, 1998; Sharma, Mantle, Gladden, & Winterbottom, 2001).

### 2.2.2. Laser Doppler anemometry and derived techniques

The principle and the main applications of LDA are well known and well described, e.g. in the excellent review of Chaouki et al. (1997): if there is a relative motion between a wave source (laser) and a wave receiver (seeding particle of the liquid or bubble in the liquid), there is a shift of wave frequency; this phenomenon is called the Doppler effect; measuring this frequency shift by using interference fringes gives access to the velocity. This technique has been applied to the determination of local velocities for some time.

LDA yields well-localised values of velocity; the measurements are very fast, allowing to determine velocity fluctuations. The last years have seen the application of LDA to the determination of liquid velocities (average values and fluctuations) in bubble columns with quite high gas throughputs (Müdde, Groen, & van den Akker, 1997; Becker, De Bie, & Sweeney, 2000; Vial, Lainé, Poncin, Midoux, & Wild, 2001a; Vial, Poncin, Wild, & Midoux, 2001b; Joshi, 2001).

Fig. 6 shows the velocity signal obtained by Müdde et al. (1998) as a function of time in a bubble column. In this figure, one of the problems of the technique becomes apparent: during a part of the measuring time, the laser beams do not reach the place where the liquid velocity is supposed to be measured, because bubbles interrupt the beam path. In Fig. 7 the RMS of the axial liquid velocity in a bubble column as measured by Vial et al. (2001a, b) is presented. The results correspond to two different gas distributors.

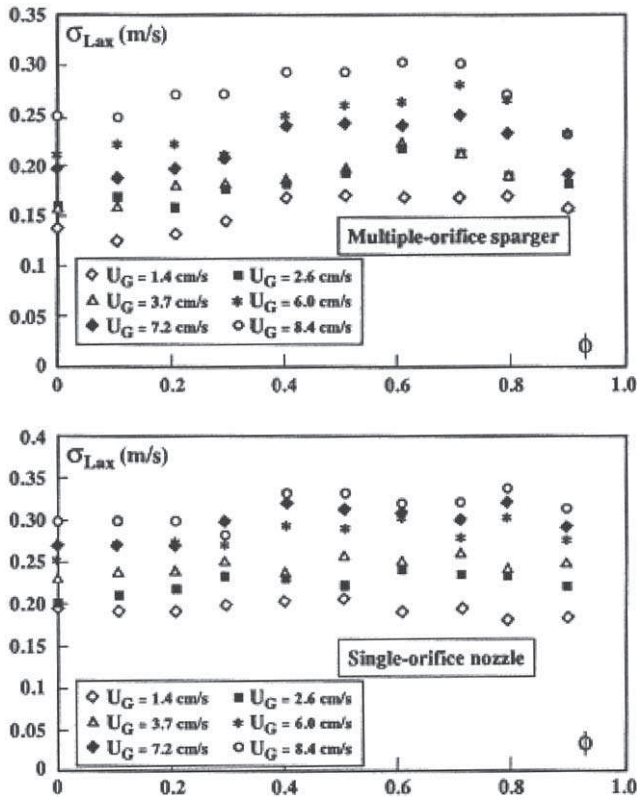


Fig. 7. RMS of the LDA-measured axial velocity in a bubble column (Vial et al., 2001a, b)

With coalescing liquids, it is possible to make reliable measurements at a distance of 0.1 m of the wall at gas holdup up to 10% (Müdde et al., 1997). At higher gas velocities, it may happen that the smaller bubbles be not distinguished from the seeding particles. This can be overcome by using fluorescent seeding particles and by using a colour filter, suppressing the incident light wavelength, but transparent to the light emitted by fluorescence (Bröder et al., 2000). Another pitfall may also be encountered: one of the basic assumptions of LDA is that the seeding particles move exactly with the liquid. However, the distribution of fine particles in the presence of bubbles may not necessarily be homogeneous in the whole of the liquid phase: over-concentrations of particles in the immediate vicinity of bubbles have been observed (Fan & Tsuchiya, 1990; Roizard, Poncin, Lopicque, Py, & Midoux, 1999). Liquid velocities measured by LDA may therefore be “contaminated” by bubble velocities. An example of such a contamination has been observed by Bendjaballah-Lalaoui (2000) and is represented in Figs. 8 and 9. In this figure, the slip velocity in the axial direction in the riser of an airlift is represented as a function of the radius, the parameter being the gas superficial velocity. The slip velocity is obtained as the difference of the time-averaged linear gas velocity  $v_{G,USDA}$  (measured by means of a ultrasound reflection Doppler probe) and the time-averaged liquid-velocity  $v_{L,LDA}$  measured by LDA. While at the lowest values of the gas superficial

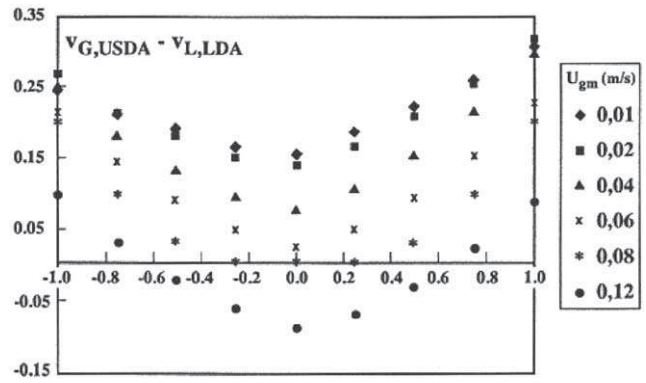


Fig. 8.  $v_{G,USDA} - v_{L,LDA}$  in the riser of an airlift reactor (Bendjaballah-Lalaoui, 2000).

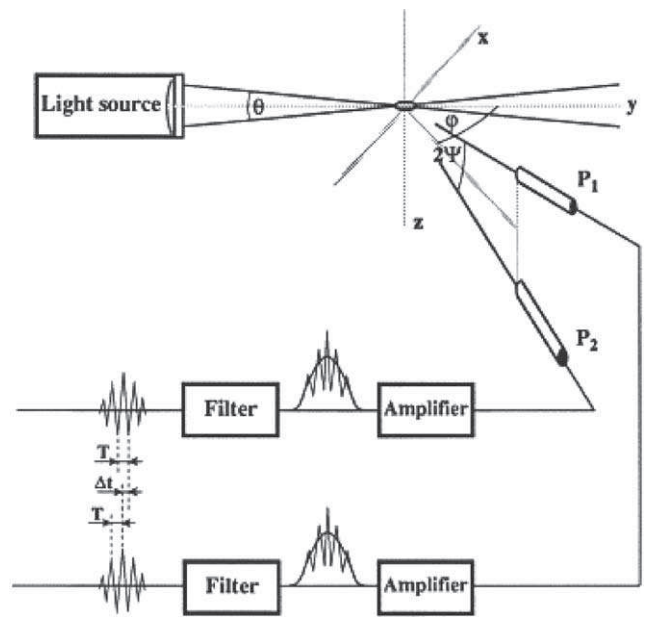


Fig. 9. PDA equipment (Bauckhage, 1996).

velocity, the slip velocity determined this way looks reasonable, at the higher values, negative slip velocities are observed, which does not make any sense in a structured flow as the one existing in the riser of an airlift. The explanation proposed by Bendjaballah-Lalaoui is that it is probable that there is a systematic error in the measurements of  $v_{L,LDA}$  with a dense bubble packing by LDA (overestimation) and another systematic error in the bubble velocity measurements (the largest and fastest bubbles may have been missed).

In phase Doppler anemometry (PDA), the Laser-Doppler signal is measured by two sensors; knowing the geometry of the system, the phase difference between both signals is directly related to the size of the particles. Fig. 8 shows the schematic principle of this technique according to Bauckhage (1996). The light emitted by the laser is divided into two beams with an angle  $\theta$  which are focused on the measuring volume, which, as in LDA can be quite small and where

interference fringes are produced. Two photodetectors are placed in a plane situated at an angle  $\varphi$  from the incoming laser beams and containing the main direction of the flow to be studied. The photodetectors are collimated on the measuring volume; their angle is  $2\Psi$ . When a spherical bubble crosses the measuring volume, bursts are observed (amplified and filtered) by both detectors. The Doppler shift can be measured as in classical LDA which yields the bubble velocity. The principle of PDA relies on measuring also the phase difference  $\Delta\Phi$  between the signals measured by the photodetectors, which is proportional to the ratio of the time lag  $\Delta t$  between the interference fringes measured with both detectors and the time  $T$  between two subsequent interference fringes as measured with either one of the detectors:

$$\Delta\Phi = 2\pi \frac{\Delta t}{T}. \quad (1)$$

This phase difference  $\Delta\Phi$  is proportional to the bubble diameter  $d$  according to the following equation:

$$d = \frac{1}{2b} \left( \frac{\lambda}{\pi n_c} \right) \Delta\Phi, \quad (2)$$

where  $\lambda$  is the wave length of the light wave,  $n_c$  the refractive index of the continuous phase (the liquid) and  $b$  a characteristic of the geometry of the system and (in the case of signals produced by refraction by the dispersed phase), by the ratio of the refraction indices of both phases. When the measured signal corresponds purely to light reflected by the bubbles,  $b$  can be calculated by the following equation:

In case of refracted light, the expression is more complicated and can be found in [Bauckhage \(1996\)](#) who gives a thorough review of this measuring technique, its advantages and problems: most applications concern liquid in gas systems; first applications to bubble columns have been made by the team of Sommerfeld ([Bröder et al., 2000](#)). However, the application is up to now limited to spherical bubbles with diameter below 1.5 mm at low gas holdup.

### 2.2.3. Polarographic technique

Polarography can be used to measure local wall shear stress. This method is based on the fast electrochemical reduction of reagent dissolved in the moving medium (Coeuret and Storck, 1984). The electrochemical system is most often the reduction of hexacyanoferrate III to hexacyanoferrate. Electrode potential is adjusted so that the reagent concentration on electrodes is zero. In these conditions, the mass transfer on each probe depends only on local hydrodynamic parameters. A simple model ([Reiss & Hanratty, 1963](#)) expresses local wall shear stress  $\tau_w$  versus delivered current  $I$  in a law of the type:

$$\tau_w = CI^3. \quad (3)$$

In bubbly flows, the polarography technique is still valid. As shown by [Souhar \(1987\)](#), a liquid film of 20  $\mu\text{m}$  thickness

exists near the wall, which enables mass boundary layer development. It has been used in bubble columns by [Magaud, Souhar, Wild, and Boisson \(2001\)](#) and at the wall of trickle beds by a number of authors (e.g. [Latifi et al., 1992](#); [Rode, Midoux, Latifi, & Storck, 1994](#)). Recently [Lesage \(2000\)](#) adapted this microelectrode technique to measurements at the surface of solid particles in trickle beds.

The advantages of this technique are twofold: it is one of the only non-invasive techniques yielding information on the flow behaviour in the immediate vicinity of the wall; it can be miniaturised (microelectrodes) and give also information on velocity fluctuations near the wall. It presents, however, a disadvantage: a conducting liquid is required and the presence of the support electrolyte can change the coalescence behaviour of the liquid.

### 2.2.4. Radioactive tracking of particles

Liquid mixing in bubble columns was investigated by the team of Dudukovic ([Dudukovic et al., 1991](#); [Chen et al., 1999](#)) using single neutrally buoyant spheres containing radionuclides emitting  $\gamma$ -rays. The use of radioactive emitting tracers is also the basis of the radioactive particle tracking (RPT or CARP) technique used by the team of Chaouki to investigate mixing of the solid in three-phase fluidised beds ([Cassanello, Larachi, Marie, Guy, & Chaouki, 1995](#); [Larachi et al., 1995](#); [Chaouki et al., 1997](#)). In the techniques proposed by both teams, the rays emitted by the tracer particle are followed by a number of detectors around the column. The reliable and rapid determination of the position of the particle from the signals obtained by all the detectors is a demanding task since a long and complicated calibration procedure is required, but it has been solved by both teams. The results of these techniques are trajectories of the particles. These trajectories can be used to confirm CFD calculations or to determine axial dispersion coefficients of the solid; on the other hand, long-term averages of the velocity yields global circulation patterns.

### 2.2.5. Tomographic techniques

The tomographic techniques have been fully developed during the last 20 years, first for medical application and more recently for industrial process application. These techniques are powerful since they give the opportunity to get the phase fraction distribution inside a reactor or a column by a totally non-intrusive measurement. The general principle consists in measuring through the column a physical property that can be related to the phase fraction. Measurements are performed at different angular positions and deliver the average values of the property over the corresponding diameters. By using a reconstruction algorithm, the acquired signals are then analysed to provide the phase fraction image on a cross-section of the column. Depending on the kind of physical property used, time and space resolution may differ widely. For tomographic systems that need to have a complete rotation of sensors all around the column, the

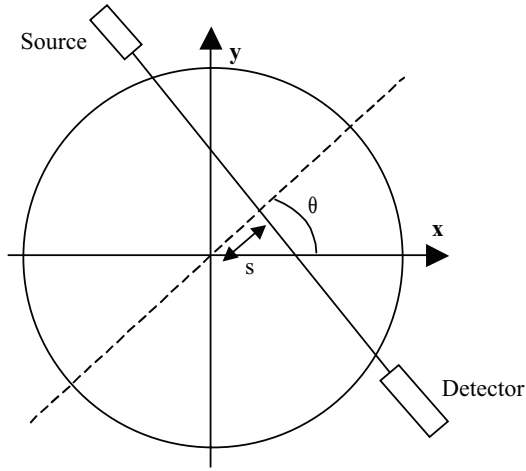


Fig. 10. Coordinates describing a measured projection.

measurements are not simultaneous and the results are only time-averaged results. Different kinds of tomographic systems have been developed.

(a) *Tomography by photon attenuation measurement.* This tomography system is based on the attenuation measurement of photon rays such as  $\gamma$ - or X-ray. This attenuation being directly proportional to the material density for a given energy, the resulting image gives the density at each pixel and then the phase fraction map. The reconstruction algorithms are based on the inversion of 2D Fast Fourier Transform since all the measured attenuations are linear functions of density. The main one is a filtered back-projection algorithm (Shepp & Logan, 1974; Kak & Slaney, 1987). If  $f(x, y)$  is the distribution function of a phase fraction inside the column, the measured attenuation corresponding to a projection of attenuation is expressed, for a given angular position  $\theta$  and a given distance  $s$  from column axis (Fig. 10), by the following relation:

$$p(s, \theta) = K \ln \left( \frac{I}{I_0} \right) = \int_{L_{s,\theta}} f(x, y) dl, \quad (4)$$

where  $I_0$  and  $I$  are the photon flux, respectively, measured, at cylindrical coordinates  $s$  and  $\theta$ , when the column is filled with one phase (liquid or gas) and when it is crossed by two-phase flow.  $K$  is a constant taking into account the relation between phase fraction and physical attenuation.

If  $P(S, \theta)$  is the one-dimensional Fourier transform of  $p(s, \theta)$ , the function  $f(x, y)$  can be reconstructed by simply taking the inverse Fourier transform of  $P(S, \theta)$ :

$$f(x, y) = \frac{1}{4\pi^2} \int_0^\pi \int_{-\infty}^{\infty} P(S, \theta) |S| e^{jS(x \cos \theta + y \sin \theta)} dS d\theta. \quad (5)$$

Instead of  $|S|$  a filter function can be used. Shepp and Logan (1974) proposed the following filter function  $g(S)$ :

$$g(S) = \frac{\delta}{2\pi} \left| \sin \left( \frac{\pi S}{\delta} \right) \right|, \quad (6)$$

where  $\delta$  is the sampling frequency.

X-ray tomographic systems have been applied to different packed beds (Schmitz & Mewes, 1997; Toye, 1996). The photon fluxes being very high with X-ray tube, the detector sensing area is quite reduced and the spatial resolution can be as small as  $1 \times 1 \text{ mm}^2$ . However, such photon rays have generally a rather low energy level (less than 100 keV) and their use is limited to low attenuating material or to small column diameter. With  $\gamma$ -rays, the photons are more penetrating since their energy can be as high as 1 MeV. Several  $\gamma$ -ray tomographic systems have been devoted to the investigation of packed beds or bubble columns (Kumar, Moslemian, & Dudukovic, 1995; Froystein, 1997). In these types of tomographic systems, the spatial resolution is rather lower (around  $1 \times 1 \text{ cm}^2$ ) but remains very interesting. It must be noted that the measurement time is directly dependent of the source activity and remain high (up to several hours for a whole measurement in industrial conditions). The  $\gamma$ -ray tomographic system must then be used with rather stationary flows.

(b) *Electrical tomographic system.* A lot of work has been done to develop tomographic systems based on impedance measurements at the wall of a column, a tank or pipe including multiphase flows (Mann et al., 1997; Reinecke & Mewes, 1997). These techniques are easy to implement with relatively low cost. Their characteristic response dynamics is very fast, they can therefore reliably describe rapid evolutions of flows. Nevertheless, the measured signal is a non-linear function of the phase fractions and of the flow configuration: the electric capacity or resistance between two separate elements at the wall depends on the whole phase repartition in the column, not only on the phases present on a straight line between the two elements. The reconstruction calculations are not easy to perform and not yet totally satisfying; the spatial resolution remains very poor unless a priori knowledge is included in the reconstruction procedure. Nevertheless, these tomographic techniques give a good information on large inhomogeneity inside a vessel or a column and they are quite adapted to detect flow configuration changes. They have been used for bubble columns (Schmitz & Mewes, 2000), three-phase monoliths and trickle beds (Reinecke, 1996; Reinecke & Mewes, 1997; Reinecke, Petritsch, Schmitz, & Mewes, 1998; Marcandelli, Lamine, Bernard, & Wild, 2000).

An interesting tomographic system has to be mentioned: two planes of conducting wire grids have been settled within a pipe (Prasser, Böttger, & Zschau, 1998). By analysing the impedance at all cross points of grids, this system is able to detect the gas fraction distribution with both a high frequency (up to 1000 frame by second) and a good spatial resolution (up to 1000 pixels). However, the system becomes invasive and is limited to flows in which the continuous phase is a conductive medium ( $\sigma \approx 0.5 \text{ } \mu\text{S/m}$ ).

(c) *Ultrasonic tomography.* Some work has been done using ultrasonic transducers to obtain tomographic images through a cross-section: ultrasonic wave propagation depends on both the phase fraction and on the phase configura-

Table 2  
Classification of invasive techniques

Techniques	Applications	Expected results	Limitations	Spatial resolution	Time resolution
Needle probe	Mainly gas–liquid, but gas–liquid–solid also	<ul style="list-style-type: none"> <li>• Gas holdup</li> <li>• Bubble velocity</li> <li>• Bubble chord distribution</li> <li>• Size distribution →</li> <li>• Bubble shape →</li> <li>• Interfacial area</li> </ul>	<ul style="list-style-type: none"> <li>• Low solid hold-up</li> <li>• Not adapted to wall vicinity</li> <li>• Adapted fluid (conductive liquid for impedance probes)</li> <li>• Model required</li> <li>• Multiple tip probes: reconstruction needed</li> </ul>	++	++
Heat transfer probe	Mainly gas–liquid, but gas–liquid–solid also	<ul style="list-style-type: none"> <li>• Gas holdup</li> <li>• Liquid average velocity</li> <li>• Liquid RMS velocity</li> </ul>	<ul style="list-style-type: none"> <li>• Low solid holdup</li> <li>• Liquid phase homogeneous in temperature</li> <li>• Adapted signal analysis required</li> <li>• Not adapted to small velocities</li> </ul>	++	++
Ultrasound probe	G–L and G–L–S	Gas holdup or interfacial area	Low gas holdup (< 20%)	+	+
• Attenuation technique	→	Bubble diameter or bubble velocity	• Spherical bubbles	+/-	+
• Doppler technique			• Small distance measurements		
Pitot tube	G–L and G–L–S	<ul style="list-style-type: none"> <li>• Flow direction or</li> <li>• Pressure drop</li> <li>• Liquid velocity</li> </ul>	Moderate gas holdup	-/+	-/+

ration (flow regime, size of dispersed particles). A very interesting work has been done by [Warsito, Ohkawa, Kawata, and Uchida \(1999\)](#) to combine the measurement of ultrasonic wave attenuation and propagation velocity to detect the solid and gas-phase fractions inside a slurry bubble column. An array of ultrasonic emitters and receivers disposed in parallel configuration at the column wall is rotated all around the column. As shown by these authors, at high frequency the wave propagation velocity does not depend on gas fraction. The solid fraction is therefore determined from the ultrasonic propagation velocity and the gas fraction is obtained by interpreting the measurement of ultrasonic wave attenuation. The authors obtained cross-section images of phase fractions using a reconstruction procedure performed with a filtered back projection algorithm. The results are quite interesting but it must be kept in mind that this application is limited to holdup fractions of dispersed phases (solid and gas) below 20%, since wave reflections on gas and solid interface rapidly generate a strong attenuation.

### 3. Invasive techniques

Although optical techniques and tomography are intensively developed for the analysis of bubble flows, invasive

measuring techniques (Table 2) cannot be avoided; yet, this is particularly true for highly turbulent systems, due to two main reasons:

- In case of nearly industrial operating conditions (particular physico-chemical characteristics, opaque walls, high gas holdup, etc.), non-invasive techniques become ineffective because of walls (as for image analysis technique), bubble number density (as for laser Doppler anemometry or Particulate Image Velocimetry), and non-stationary phenomena: non-invasive techniques usually offer discrete or time-averaged data, making thus statistical or spectral analysis impossible or cumbersome.
- non-invasive techniques are often not easy to apply and are often quite expensive!

The main invasive methods for local measurements appeared in the early 60s, before the development of experimental non-invasive hydrodynamic techniques: searchers involved in experimental work observed quite early the intense non-homogeneous and non-stationary characteristics of most gas/liquid flows. In the 70s, non-stationary phenomena analysis was conducted through invasive techniques development; [Jones and Delhaye \(1976\)](#) wrote one of the first reviews this topic, while [Serizawa, Kataoka, and Mishigoshi](#)

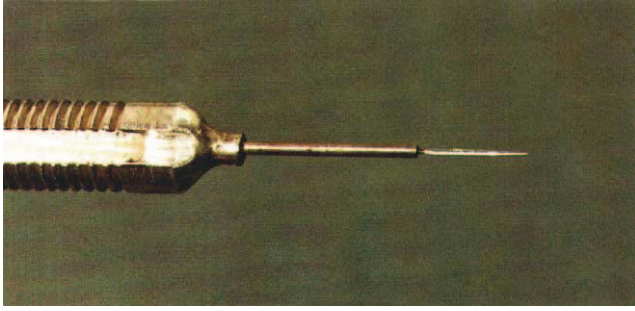


Fig. 11. Optical needle probe (RBI, 1996).

(1975) published the first article (a priori) on complete experimental investigation of both gas and liquid phases in two-phase flows.

### 3.1. The so-called 'needle probes'

These probes are very thin, sharp ended; they are settled to face flow direction, in order to pierce as many bubbles as possible. Needle probes are used to study high gas holdup systems (Nicol & Davidson, 1988; Utiger, Stüber, Duquenne, Delmas, & Guy, 1999; Bentifraouine, 1997). In some cases, they allow a complete description of gas phase hydrodynamic characteristics. Two main types of needle probes can be distinguished:

- optical fibre probes (Fig. 11)
- resistive or conductive probes, or even more generally 'impedance probes'.

Needle probes are used as single-tip or double-tip systems, depending on the kind of data expected: single-tip probes lead to gas fraction, and bubbling frequency; double-tip probes allow measurements of bubble velocity, time-average local interfacial area, and mean bubble chord length.

#### 3.1.1. Principle

(a) *probes and corresponding electronic device.* Optical probes are made in quartz (Jones & Delhaye, 1976), and usually protected by a protective layer except at the tip (1 cm long) to allow measurements. The sensing tip can be also made in sapphire for measurement in aggressive environment (e.g. in a three-phase fluidised bed as in Bigot et al., 1990). Probe tip diameter is usually smaller than 200  $\mu\text{m}$  and sometimes 50  $\mu\text{m}$  (Groen, Mudde, & van den Akker, 1995).

In the case of an optical probe, an infra-red light beam is guided along the fibre to its tip. The fibre usually ends with a thin conical tip to correctly pierce bubbles. Following optic laws, this tip transmits the light beam when in liquid medium, or reflects it back (towards the electronic device) when it is surrounded by gas (Chabot, Farag, & De Lasa, 1998; Choi and Lee, 1990). An opto-electronic device (pho-

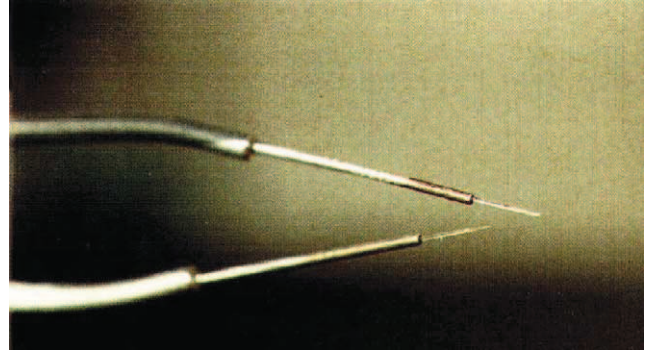


Fig. 12. Double-tip optical probe (RBI, 1996).

totransistor) delivers an analog output signal in proportion to received light intensity.

Impedance needle probes are very similar to optical ones. They are made of metal wire (stainless steel, nickel, corundum, platinum (e.g. Fröhlich et al., 1991; Hogsett & Ishii, 1997) thus resisting to oxidation. Their diameter ranges from 2.5 mm to 50  $\mu\text{m}$ , reaching 12  $\mu\text{m}$  in case of surgery needles (Thang & Davis, 1979; Nakoryakov, Kashinsky, & Kozenko, 1984). They are embedded within a metal support.

An impedance probe behaves as an electrode (Jones & Delhaye, 1976; Liu, 1993). A potentiometer (around 100 k $\Omega$ ) measures the difference in voltage between the probe and the support, the latter being usually grounded (Hogsett & Ishii, 1997).

(b) *Double probes.* Double probes, or 'biprobes', need a tiny distance between the tips (some 0.5–5 mm) (Chabot et al., 1988; Moujaes & Dougall, 1987; Chen, Zheng, Feng, & Hofmann, 1998; Kang, Cho, Woo, Kim, & Kim, 2000) minimising the risk for a bubble which has been pierced by the front tip, to miss the rear one. A sufficiently high number of bubbles identified by both fibres allows a realistic statistical treatment for gas-phase hydrodynamic parameters. Of course probe tips have to be aligned with bubble rise direction (Fig. 12).

Some special optical probes (Cartellier & Achard, 1991), based on needle probe operation principles, have been developed in laboratories.

- probes bent in a U shape tip (Jones & Delhaye, 1976; Lee & De Lasa, 1987; Yu & Kim, 1991). Such probes are however extremely fragile and are, to the knowledge of the authors, no longer in use,
- probes with melt extremities, giving a spherically shaped tip (Moujaes, 1990; Chabot, Lee, Soria, & De Lasa, 1992; Chabot & De Lasa, 1993).

Some authors proposed multiple (3–7) point probes (Brück & Hektor, 1984, Buchholz, Tsepetonides, Steinemann, & Onken, (1983); Buchholz, Zakrzewsky, & Schügerl, 1981; Burgess & Calderbank, 1975; Jakobsen, Svendsen, & Hjarbo, 1992; Svendsen, Luo, Hjarbo, &

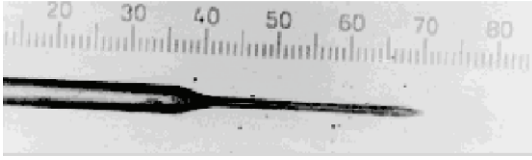


Fig. 13. Shape of A. Cartellier's single fibre optical probe.

Jakobsen, 1998; Wolff, 1989; Wolff, Briegleb, Bader, Hektor, & Hammer, 1990; Yao, Zheng, Gasche, & Hofmann, 1991). A number of such devices are to be found in the review of Lübbert (1991). It is possible with such probes, at least in principle, to determine the full set of components of the velocity vector, regardless of its direction, and the bubble diameter. There are however practical problems limiting the use of such devices: the probes rapidly become bulky and so hydrodynamic interaction between bubbles and the probe cannot any longer be neglected; furthermore the exploitation software is far from easy to develop.

It is worth mentioning that Cartellier's group (Laboratoire des Ecoulements géophysiques et Industriels: LEGI, Grenoble) developed an original single-fibre optical probe; this probe is constituted of conical and cylindrical parts (Fig. 13), leading to a specific type of registered signal; this allows the simultaneous measurement of several gas-phase characteristics, just like a double probe: local gas holdup and interface velocities (Cartellier, Poupot, Chambérod, & Barrau, 1996; Cartellier, 1992; Barrau, Rivière, Poupot, & Cartellier, 1999). By detecting the transit time of the bubble interface between the probe tip and the end of cylindrical part, it is possible to intrinsically deduce the bubble velocity. A specific application of this probe will be described in Section 4.1.3.

(c) *delivered signal*. Basic principles for needle probes operation being stated, it is easy to understand that the associated electronic device delivers a signal varying between two bounding levels; these levels depending on the phase surrounding the tip of the needle (gas or liquid); bubble-probe interaction and bubble detection have been extensively described in literature (Lübbert, 1991; Groen et al., 1995; Cartellier et al., 1996; Cartellier & Barrau, 1998; Cartellier, 1992; Barrau et al., 1999).

In order to correctly describe signal variations between the two limiting levels, a high sampling frequency is required: 1–10 kHz, or even 1 MHz for real time sampling.

The acquired signal is then binarised (Revankar & Ishii, 1992; Hogsett & Ishii, 1997). Trigger level choice may obey various criteria (Jones & Delhaye, 1976; Young, Carbonell, & Ollis, 1991). A frequently used trigger to get rid of noise corresponds to 10% of bubble passage typical signal rise.

### 3.1.2. Measuring results

Time-averaged gas holdup and bubbling frequency are directly reached through straight forward signal analysis (Liu, 1993).

With a double-tip probe, two signals are simultaneously registered. The cross-correlation function between both signals leads to the most probable delay needed by a bubble to migrate between the two tips (Revankar & Ishii, 1992). The most probable bubble mean axial velocity is then derived (Roig, Suzanne, & Masbernat, 1998; Moujaes & Dougall, 1987). As mentioned earlier, a bubble can reach the front tip and miss the rear one; a criteria is therefore required to associate signal pulses caused by the same bubble on both tips (Revankar & Ishii, 1992).

To evaluate the specific time-averaged interfacial area, some authors suggest a relation that takes mean bubble velocity  $\bar{V}_b$  and bubble frequency  $N_t$  into account (Kataoka, Ishii, & Serizawa, 1986; Revankar & Ishii, 1992; Dias, França, & Rosa, 2000) in the case of spherical shape bubbles (less than 5 mm in diameter) and for quiet bubbling regime: the product ( $2N_t \frac{1}{\bar{V}_b}$ ) is consistent with the interfacial area. A correction factor, based on RMS fluctuation  $\sigma_z$  of axial velocity component, is also used (Kataoka et al., 1986; Dias et al., 2000). Authors assume  $\sigma_z$  to be equal to velocity components RMS fluctuations in the other direction.

Going back to raw signal bubble pulse width, and using calculated bubble velocity, it is possible to obtain the corresponding chord size along which the probe tip has pierced the bubble. The local bubble chord length distribution can then be derived (Yu & Kim, 1991). Its first momentum is the mean chord length  $\bar{C}$ .

Through reverse transform of local bubble chord distribution, it is possible to get the probable corresponding local diameter distribution, by assuming an homogeneous bubbling regime and spherical shape for bubbles (Uga, 1972), and by using a proper statistical law (Clark & Turton, 1988). This analysis has been extended to ellipsoidal shaped bubbles by Kamp, Colin, and Fabre (1995); and to heterogeneous bubbling regime by Liu, Clark, and Karamavruc (1998). The precision is however less satisfactory in the later cases.

It is worth noting that, in the case of an infinitely small probe tip, the mean bubble diameter  $\bar{D}$  is easily deduced from the mean bubble chord  $\bar{C}$  (Thang & Davis, 1979; Moujaes & Dougall, 1987; Fröhlich et al., 1991):  $\bar{D} = k\bar{C}$ .

If bubble shape is perfectly spherical,  $k$  is equal to 1.5; otherwise, it has to be experimentally optimised (Fröhlich et al., 1991).

### 3.1.3. Technique limitations

The application of needle probes is limited by some physical problems. It is evident, e.g., that, in order to yield reliable results, the probe tip has to be very thin compared with the mean dimension of the bubble population studied. The following other drawbacks are encountered: optical needle probes do not operate in all organic liquids because of a too small difference in refraction index with the gas phase. Organic liquid conductivity is also too small for the use of impedance probes; in the case of low-conductivity aqueous

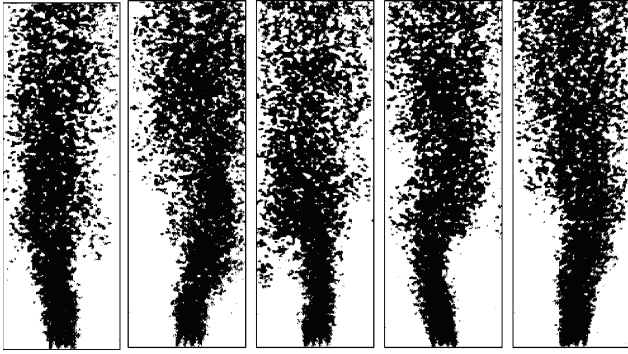


Fig. 14. Oscillating bubble plume (Salesse et al., 2001).

medium however, some salt may be added to allow reliable measurements.

The following factors intrinsically linked to the measuring method may reduce its accuracy:

- errors due to bubble-probe interaction: piercing hydrodynamics (which depend on probe surface quality among other parameters) (Hogsett & Ishii, 1997; Cartellier et al., 1996), probe orientation in flow (Groen et al., 1995), bubble shape (for non-spherical bubbles, evaluation of sizes and of interfacial area is often questionable (Buchholz et al., 1981)); multiple point conductivity probes are then to be preferred),
- errors due to flow characteristics: turbulence, non-stationary phenomena (Groen et al., 1995),
- statistical bias: in a given area around the probe tip, large bubbles are more likely to be pierced than small ones (Thang & Davis, 1979),
- errors due to signal treatment: critical trigger choice for bubble identification (Nakoryakov, Kashinsky and Kozenko, 1984; Serizawa et al., 1975).

### 3.1.4. Illustration of needle probe application

The recent work of Salesse, Larue de Tournemine, and Roig (2001), dedicated to the analysis of an oscillating bubble plume, is a spectacular illustration of needle probe application.

A plume of fine bubbles has been specifically generated within a rectangular vertical tank by means of capillary tubes; the typical gas flow rate is  $11.6 \times 10^{-5} \text{ m}^3/\text{s}$  (superficial velocity: 4.9 mm/s). This plume oscillates in the transverse direction (Fig. 14) with a mean frequency of 0.235 Hz.

The bubble plume envelope is characterised by means of a series of 10 resistive single-tip probes (regularly spaced with 1 cm distance). Each probe delivers a phase function in a 2500 s long signal which is binarised and plotted versus time (Fig. 15).

An iterative algorithm, derived on the basis of the correlation between phase function matrix and an assumed model, leads to a rather precise representation of bubble swarm frontiers. This procedure is currently being gener-

alised by these authors to flows showing random bubbling regime.

## 3.2. Heat transfer probes

To describe experimentally the liquid phase within two-phase flow with moderate gas holdup, hot film anemometry is more and more often used (this invasive technique had been developed for single-phase flow for a long time).

Hot film anemometry, when applied to two-phase flows, leads to gas fraction and to liquid-phase characteristics: mean velocity and RMS fluctuating velocity.

### 3.2.1. Basic principles

(a) *interaction between probe and surrounding flow.* Hot film anemometry is based on the heat exchanged between an electrically heated probe and the surrounding liquid medium. Following King (1914), pioneer of hot probe anemometry, the convective heat transfer coefficient between a probe and the surrounding fluid depends on the characteristic Reynolds number and can be described by:  $Nu = A + B Re^{-0.5}$ .

Electric current through the probe, and so hot film resistance, are controlled by a Wheatstone bridge associated to a regulation amplifier and a high-pass filter.

(b) *calibration.* The relation between the probe voltage  $E_w$  and the liquid velocity is King's law (Utiger et al., 1999):  $E^2 = A + B U_e^n$ , where,  $A$ ,  $B$  and  $n$  are coefficients to be identified;  $U_e$  is the apparent fluid velocity (whereas the actual velocity is  $U$ , vector), sensed by probe. In the case of a non-uniform flow,  $U_e$  is the normal component of  $U$  with regards to the probe.

The coefficients  $A$ ,  $B$  and  $n$  of King's law depend a priori on physical properties (density, viscosity, thermal conductivity) of the fluid near the probe, but also on geometric characteristics of the sensor. These parameters may also vary with the difference in temperature between the hot film and the fluid (Bruuns, 1995).

Calibration of the probe (i.e. determination of the parameters of King's law) is done by a reference measuring technique: Pitot tubes are often chosen (Bruuns, 1995). It has to be stressed that a calibration curve has to be checked daily because sensor characteristics may change rapidly.

(c) *Probe characteristics.* The hot film probe sensitive element (Fig. 16a) is tiny (25–100  $\mu\text{m}$  thickness); it is made of a quartz substrate (thermal insulation) recovered with a platinum or nickel film, and protected from oxidation and abrasion by a quartz layer (1 or 2  $\mu\text{m}$  thickness).

In the case of multi-directional flows, two- or three-film probes are used (Fig. 16b and c).

(d) *Bubble flow measurements.* Hot film anemometry has been applied to bubble flows since the 60 s (Abel & Resch, 1978). Bubble passage on probe generates a deep drop (Fig. 17) in heat exchange and so creates a rupture of signal. This is detailed by Bruuns (1995) for the example of a cylindrical sensor.

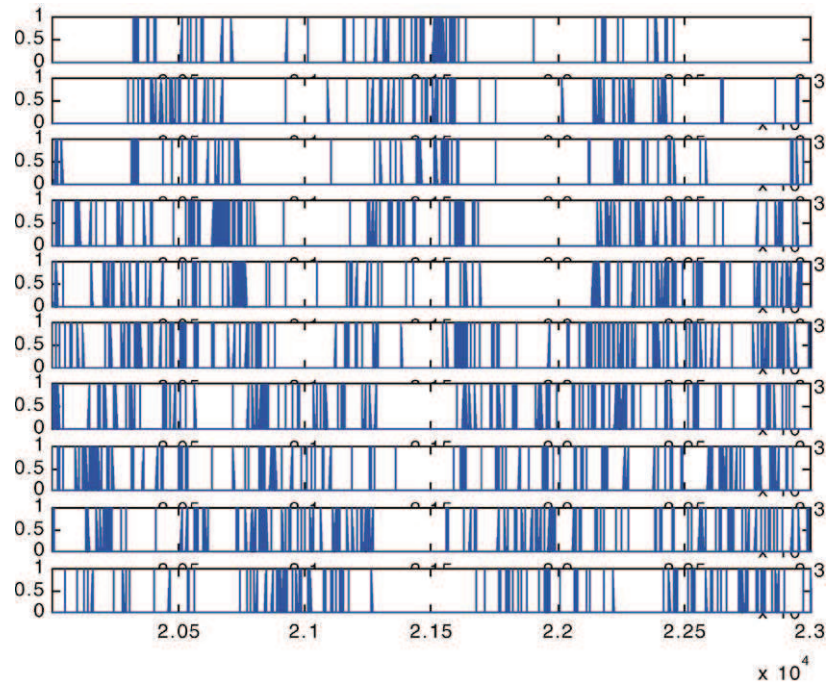


Fig. 15. Binarized phase function for simultaneous registered signals from 10 mono-tip probes (Salesse et al., 2001).

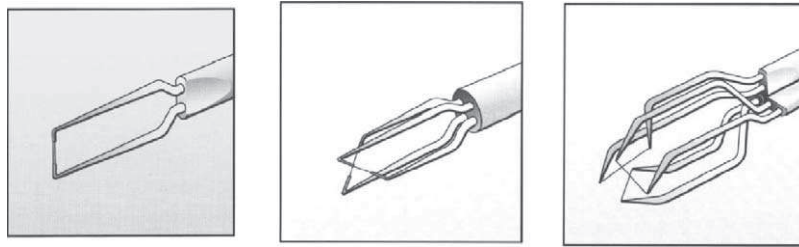


Fig. 16. Common hot film probes (Bruuns, 1995).

### 3.2.2. Measuring results

(a) *Gas-phase fraction*. The first step of signal treatment consists in identification of all bubbles. Several authors applied triggers of the signal magnitude (Delhaye (1969), mentioned by Young et al., 1991; Resch & Leutheusser, 1972; Resch, Leutheusser, & Alemu, 1974; Jones & Zuber, 1978; Toral, 1981; Farrar, 1988; Samways and Bruun, 1992; Farrar, Samways, Ali, & Bruun, 1995).

It is in fact necessary to combine triggers in both magnitude and slope (Wang, Lee, Jones, & Lahey, 1990; Liu & Bankoff, 1993; Utiger et al., 1999) to recognise bubbles. Time-averaged gas holdup may then be evaluated at probe location. The reliability of this holdup calculation has been proved in air–water medium by Utiger et al. (1999) using an independent validation technique (optic needle probe).

(b) *Liquid-phase velocity*. When the signal drops due to bubble passage have been removed, the remaining part, which corresponds to measurement within the liquid phase, can be analysed. The time-average local liquid

velocity and its RMS fluctuations are calculated using King's law.

Literature reports a few works dedicated to turbulent quantities measurements in bubble using hot film anemometry:

- the time-averaged local values: the liquid velocity is integrated over the cross-section and can be compared with the liquid flow rate in the pilot (Serizawa et al., 1975; Utiger et al., 1999);
- from RMS velocity fluctuations, turbulent quantities are evaluated and analysed (Serizawa (1974), mentioned by Jones & Delhaye, 1976; Lance & Bataille, 1983; Magaud, 2000). Hogsett and Ishii (1997) even distinguish turbulence due to bubble and turbulence due to wall friction;
- by means of a double-sensor probe, two components of liquid velocity may be simultaneously determined. Reynolds shear stress can then be deduced (Lance & Bataille, 1983; Menzel, In Der Weide, Staudacher, Wein, & Onken, 1990);

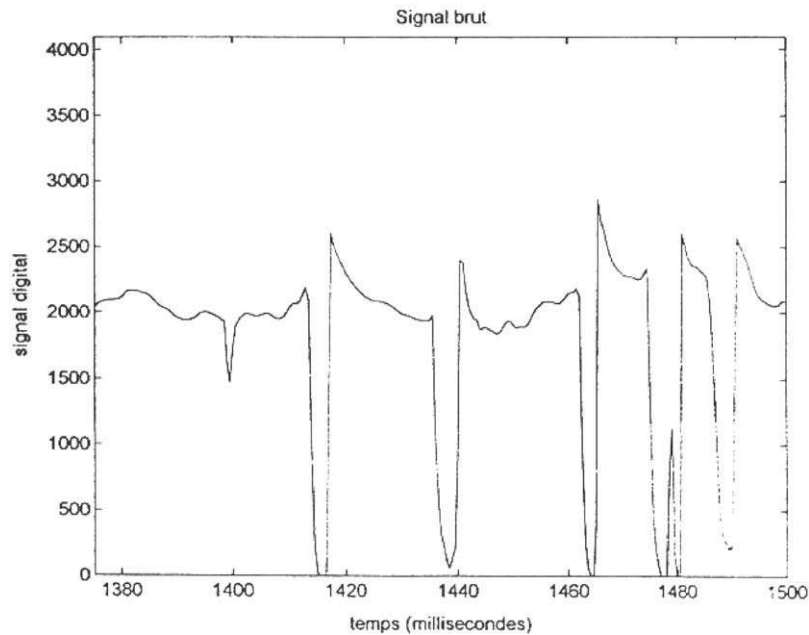


Fig. 17. Sample of hot film probe output signal.

- once parts due to bubbles have been eliminated from the signal, one can proceed to the auto-correlation function calculation, even if the remaining signal is not continuous. This function is expected to point out a characteristic frequency corresponding to turbulence time scale (Roig, Larrieu, & Suzanne, 1995). Turbulence and energy dissipation power spectra may also be determined, in the same way as with single-phase flow analysis (Schügerl, 1982):

Liquid velocity, however, is influenced by bubble rise front and bubble drag. These specific velocity fluctuations are ambiguous: some authors (Roig et al., 1998) think that they are not representative for liquid flow and that they should not contribute to turbulent quantities evaluation. These authors eliminate the corresponding parts from the signal.

### 3.2.3. Technique limitations

Hot film anemometry can be applied with many media. Caution must be taken because sensors are fragile: solid particles with high momentum have to be avoided. What is more, the flow studied has to be uniform in temperature.

Hot film anemometry is not a very expensive technique and offers good measurement accuracy (0.1 to 0.2% for rigorous experiments; this is as good as laser Doppler Anemometry) and a good signal-to-noise ratio.

No limitation in gas holdup has been notified in literature: hot film signals can be useful as long as bubbles can be distinguished. Experiments on liquid and gas phase through hot film anemometry have been carried under some 20% gas holdup (Utiger et al., 1999).

Hot film measurements errors arise from several factors: flow disturbance due to probe, calibration curve uncertainty, signal treatment, signal amplification, signal interpretation in turbulent flow and in low velocity zones, and temperature non-uniformity. The last two points are the most difficult to evaluate (Fingerson & Freymouth, 1983; Bruuns, 1995).

Mass balance, when time-average local liquid velocities are integrated over a cross-section, has been satisfied with an error of 10–21% by Young et al. (1991) and of less than 11% by Utiger et al. (1999).

Measurement accuracy is more difficult to estimate for turbulent parameters; but results are rather reproducible and Lance and Bataille (1983) state that the corresponding error is limited to 10%.

### 3.2.4. Similar or derived techniques

Many local techniques exist that are based on heat transfer principles and are similar to hot film anemometry (Young et al., 1991; Bruuns, 1995). Most of them have been specifically developed to answer the question of local reverse flows. Among them, heat pulse probes and split film probes are rather common.

The same kind of probes can be derived using mass instead of heat transfer: micro-electrodes rely on polarographic technique using a redox system: the most frequent reaction is the oxidation of hexacyanoferrate II to hexacyanoferrate III. The drawbacks are that the liquid must be a conductive solution with relatively high support electrolyte concentrations, which may induce coalescence inhibition. This drawback can be overcome by using the reduction of dissolved oxygen on a silver or gold electrode, since this technique requires a less concentrated support electrolyte

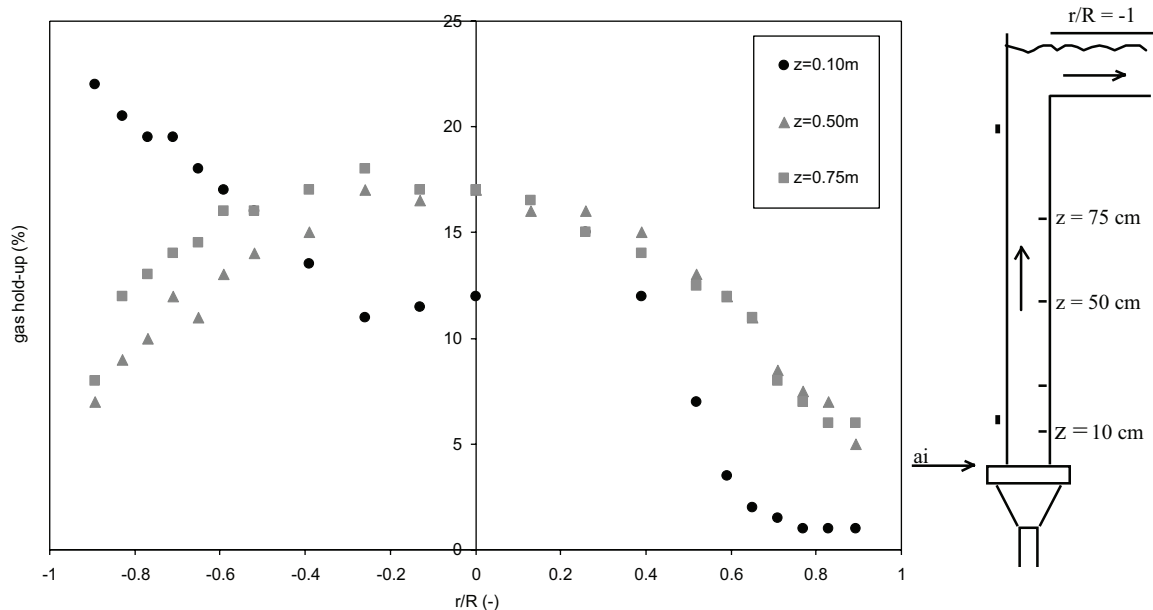


Fig. 18. Gas holdup (%) in an external loop airlift reactor (superficial gas velocity: 0.069 m/s) (Utiger et al., 1999).

(Pauli, Menzel, & Onken, 1989; Pauli, Onken, & Sobolík, 1991; Pannek, Pauli, & Onken, 1994).

As with hot film anemometry, the polarographic techniques needs a signal treatment to discriminate between bubbles and liquid (Vial, 2000). This technique however allows the investigation of mass transfer properties (Vial, 2000), and also the measurement of hydrodynamic characteristics such as liquid velocity and shear stress at the wall (Mitchell & Hanratty, 1966) or at the surface of a particle (Lesage, 2000), two-phase flow properties (Souhar, 1982; Latifi et al., 1992, 1994a, b; Rode et al., 1994; Magaud, 1999). As with thermal anemometry liquid flow direction can be measured by using probes with three or more microelectrodes (Pauli et al., 1989; Pauli et al., 1991; Pannek et al., 1994).

### 3.2.5. Hot film anemometry: example of application

Utiger et al. (1999) performed a detailed hydrodynamic map of both phases (water–air) parameters in an external loop airlift reactor (15 l). Authors used a single sensor hot film probe (DANTEC, 55R11) and a double-tip optical probe.

Figs. 18 and 19 show radial profiles of time-average and fluctuating local liquid velocities, drawn for the upper part of the riser column. Such a map of phases properties gives a good overview of the two-phase flow as well as a diagnostic of peculiar zones. In this work for instance, authors put in evidence how, at the bottom of the riser, back flow disturbs gas and liquid distribution. Going up along the riser, gas and liquid velocities develop into profiles of usual shape.

### 3.3. Ultrasound probes

Ultrasound techniques for the measurement of bubble characteristics are based on the laws of ultrasound wave

propagation in a two-phase medium. These techniques can be divided into two types:

Some use transmitted wave characteristics (attenuation): they lead to gas holdup or to time-averaged local interfacial area.

Some (Doppler techniques, for instance) use characteristics of the wave that reflected by the bubble surface: magnitude and frequency of reflected wave are measured and lead to bubble size or to bubble velocity.

Probes are similar for both kinds of technique. Transmittance techniques need an emitting probe and a receiving one, both aiming at the measuring point; US Doppler probes generally operate both as emitter and receiver.

#### 3.3.1. Probe description

The probe consists in a piezo-ceramic disk (less than 1 mm thick) linked to a damping device included in a metal tube (Fig. 20) (Stravs, Wahl, von Stokar, & Reilly, 1987; Bröring et al., 1991; Bouillard, Alban, Jacques, & Xuereb, 2001). These probes can be used in opaque, viscous and even aggressive media; they resist up to 140°C and 20 MPa (Bröring et al., 1991).

Acoustic pressure waves generate vibrations within the piezo-ceramic disk; the disk transforms them into a voltage signal transmitted to a computer via an electronic device constituted by appropriate filters.

These techniques can be applied to US signals ranging between 0.2 and 5 MHz (ultrasound wave field of frequencies begins at 20 kHz). Ultrasound wave length has indeed to be chosen significantly different from bubble size to hinder resonance phenomena. It is worth noticing that the measuring point locates at focal distance from probe (some 0.2 or 0.3 m and thus does not disturb the flow studied).

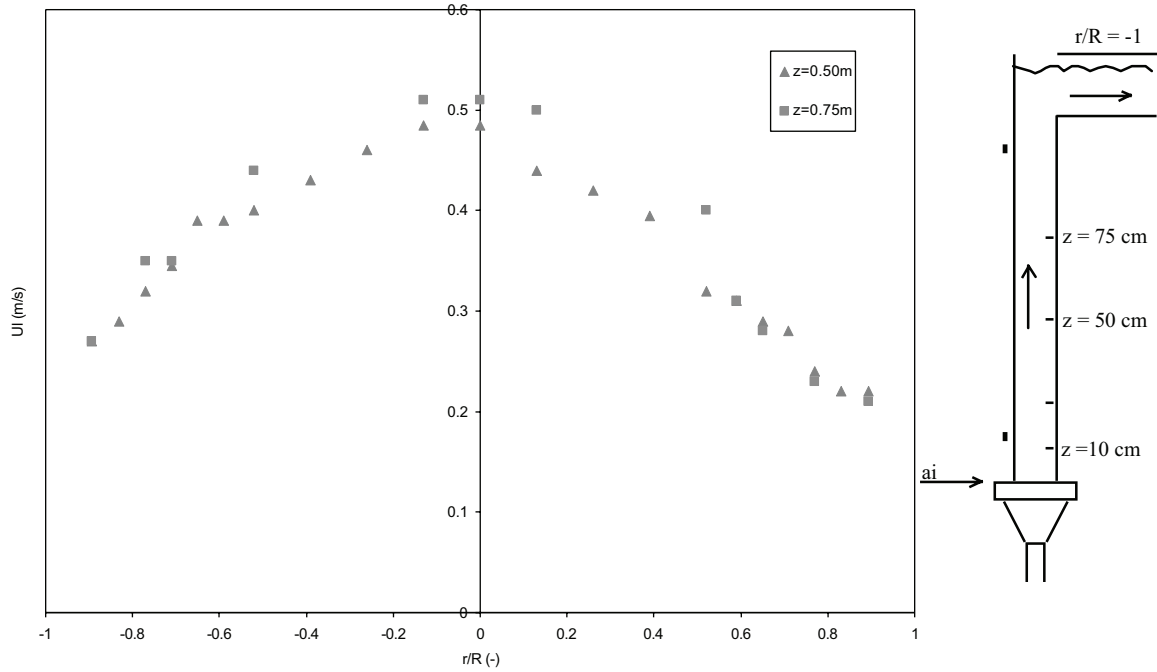


Fig. 19. Time-averaged liquid velocity (m/s) in an external loop airlift reactor (superficial gas velocity: 0.069 m/s) (Utiger et al., 1999).

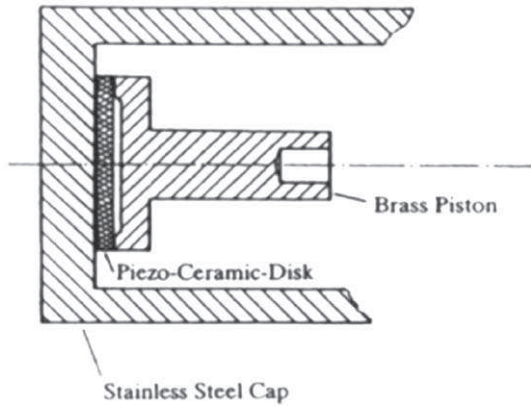


Fig. 20. Detailed cross-section view of an ultrasound Doppler probe (Bröring, Fischer, Korte, Sollinger, & Lübbert, 1991).

### 3.3.2. Principles and expected data

(a) *Ultra-sound transmittance technique (UTT)*. When emitting and receiving probes are separated by a two-phase flow, transmittance  $T$  is evaluated through the voltages  $A$  and  $A_0$  measured at the receiver probe in the presence or absence of bubbles, respectively.

$T$  depends on:

- distance  $L$  between the two probes,
- bubble size,
- bubble projected surface,
- ultra-sound wave characteristics (frequency  $f$ , celerity  $c$  in liquid medium).

A recent measuring device was developed and used by Bensler (1990) and Boyer (1996). It differs from pre-

vious studies because large frequency band sensors are used.

Knowing transmittance  $T$ , bubble Sauter mean diameter and sound dispersion coefficient  $S$ , the local mean interfacial area  $a$  or the local gas holdup  $\varepsilon$  can be calculated (Stravs & von Stockar, 1985) by measuring the transmittance  $T$  at two different frequencies:

$$a = \frac{-8 \ln(T)}{SL(kd_{SM}/2)} = \frac{6\varepsilon}{d_{SM}}, \quad (7)$$

where  $k = (2\pi/c)f$ .

(b) *Pulse echo technique*. Gas-liquid interfaces are effective ultrasound reflectors because acoustic impedance is very different in a gas or in a liquid. To analyse reflected wave characteristics, pulsed signals are often used (pulse echo technique) to filter echo through their transit delays. Note that the shorter the pulses, the weaker the echo distortion due to the contribution of other parts of the bubble (Stravs et al., 1987); thus pulse emission frequency ranges around 10 kHz.

- reflected magnitude analysis:

Focusing an acoustic beam towards a sphere holding at a distance  $L$  from the probe (some 20 mm), one obtains a bell shape profile for the echo's acoustic magnitude  $\alpha_R$  (Fig. 21):

On this graph,  $x$  co-ordinate stands for the radial position of bubble centre apart from acoustic propagation axis. Probe-bubble distance being known through US pulse migration time, one can evaluate the size of a bubble hit at  $x = 0$  by analysing this profile.

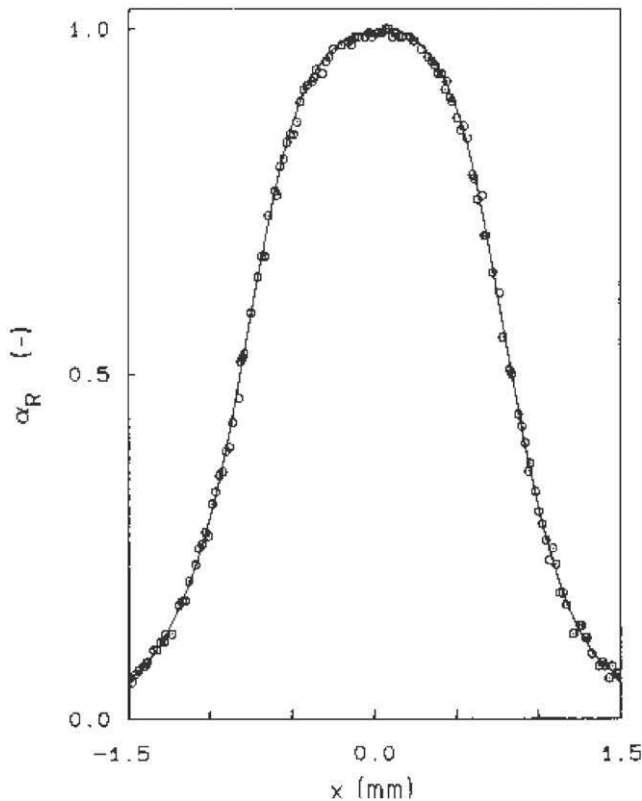


Fig. 21. Echo magnitude profile (Stravs et al., 1987).

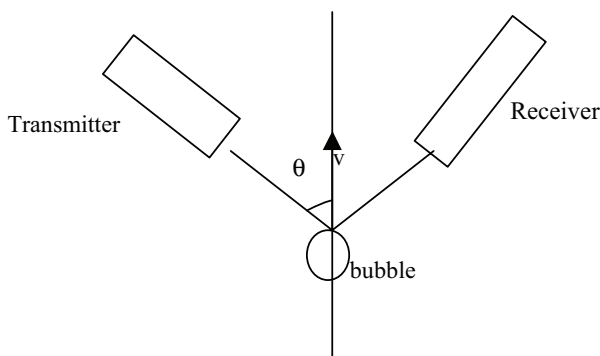


Fig. 22. US Doppler method basic principle for a both emitting and receiving probe.

- frequency analysis of the reflected wave (Doppler effect): US Doppler anemometry is based on the difference in frequency between an emitted US pulse and the corresponding received US pulse that has been reflected by a moving bubble. This well-known method leads to the local bubble velocity distribution (Bröring et al., 1991; Yao et al., 1991; Fischer, Bröring, & Lübbert, 1992; Ruffer, Bröring, & Schügerl, 1995). Its principle is shown on Fig. 22.

The investigated volume of flow is not bigger than a few cubic centimetres.

### 3.3.3. Ultrasound techniques limitations

Generally speaking, ultrasound techniques allow instantaneous measurement of only one characteristic of the dispersed phase at a time; furthermore, they are ineffective under high gas holdup conditions (more than 20%), because the acoustic signal is lost due to repeated reflections (Bröring et al., 1991).

Bubble size evaluation method (Pulse Echo Technique) can be partially extended to non-spherical bubbles but, in the case of ellipsoidal bubbles for instance, this leads to a 20% error in regard with photographic technique measurements (Stravs et al., 1987).

Note that US Doppler technique is drastically influenced by probe orientation in flow. Furthermore, when a non-focused acoustic beam is used, spatial resolution and signal-to-noise ratio become very poor as distance from probe increases. According to Bouillard et al. (2001), this technique is intrinsically less precise than Laser Doppler Anemometry, but also much cheaper.

### 3.3.4. Ultrasound techniques applications

In the work of Ruffer et al. (1995) phase distribution in an external loop airlift (60 l) equipped with static mixers and operated with viscous and non-viscous fluids (water and CMC solutions) was investigated. Bubble velocity (vertical and horizontal components) was measured by means of US Doppler technique.

These authors observe that the distribution of bubble velocity vertical component is wide and complex; velocities of large and small bubbles are shown to be very different; indeed some very small bubbles, much influenced by liquid flow, flow downwards in the column.

In horizontal direction, bubble velocity fluctuations do not depend on bubble size anymore; they are due exclusively to liquid-phase turbulence. The distribution of bubble velocity horizontal component is wider than the corresponding distribution of vertical one (for the same operating conditions); this observation shows that turbulence is not isotropic for this flow: the largest bubbles rise fast and take liquid along with them. The horizontal component of bubble velocity is drastically influenced by the passage of large and energetic eddies.

## 3.4. Pitot tubes

Pressure measurement is a robust and easy way of flow diagnosis. As it has been stated in Section 2, wall pressure transducers are widely applied nowadays, but intrusive pressure probes, so-called 'Pitot tubes', are still very useful. For bubbly flows, it may be used with an appropriate procedure. This technique is well known in the field of single-phase flows for fluid velocity measurements, so the following description will be short.

### 3.4.1. Principle

Single Pitot tubes, dedicated to velocity local measurement, should be quite thin (1–2 mm) (Davis, 1979; Nicol & Davidson, 1988; Chue, 1975) to avoid flow disturbance. Five hole Pitot tubes have been described in literature (Bruuns, 1995; Chue, 1975; Ligrani, Singer, & Baun, 1989; Cho & Becker, 1985). Various shapes are encountered: streamlined, spherical or conical; the Pitot tube may even be constituted of five parallel tubes. Each nozzle is linked to a manometer. The total pressure is read through the central hole; the other four nozzles, located all around the central one, measure static pressure. These Pitot tubes allow to measure both the liquid velocity magnitude and direction.

To perform pressure measurements in bubble flow, one has to hinder bubbles from entering the nozzles. To achieve this, Nicol and Davidson (1988) feed their Pitot tube with a liquid flow (5 cm/s), making the probe free from the disturbance due to bubbles. Caution must be taken, however, because this type of apparatus may modify flow structure around the probe.

### 3.4.2. Obtained data

There are two ways to use such Pitot tubes:

- The tubes can be rotated around their own axis to find the precise orientation for which the four external tubes deliver the same value of pressure; this particular position reveals the mean direction of the flow.
- The Pitot device can be set vertically in the flow; differences between the pressure measurements from two neighbouring holes are then investigated (right-left, up-down):
  - The difference in pressure from two lateral holes (separated by a vertical distance  $h$ ) is the difference in the local hydrostatic pressure, The local value of the apparent density of the two-phase mixture  $\rho_m$  is then calculated and leads to the local gas holdup with a relative error of some 10%.
  - The difference between total pressure and static pressure is equal to the dynamic pressure, and leads to the local liquid velocity. According to Davis (1979), dynamic pressure measurement from a Pitot tube in bubble flow gives always a larger value than expected according to the predictive laws for single-phase liquid flow, provided the Pitot probe's size is kept smaller than bubble mean diameter. A correction factor, taking the disturbing effect of relative motion of phases around the Pitot tube into account, and ranging between 1 and 1.73, is then used when measuring the local dynamic pressure. This factor however depends also on gas holdup; the maximal value of 1.73 is reached for 60% of gas holdup (Davis, 1979).

To evaluate liquid velocity by Pitot tube measurements in bubble flow, the mean density of flow,  $\rho_m$ , has thus to be previously derived: by measuring first the static pressure or the gas holdup.

### 3.4.3. Limitations of the technique

Pitot tube velocity measurements meet similar limitations as measurements made with hot film probes. Pitot tubes are thicker and the derived data correspond therefore to a less fine degree of analysis.

Pitot tubes may also be difficult to implement but they are robust and can be applied to hostile environments (when gas–liquid flow includes solid particles). Nicol and Davidson (1988) estimate the error made on liquid-phase mean velocity measurement to some 4%.

As mentioned before a calibration is still needed when used in bubble flow to take into account of bubble slip velocity in the vicinity of Pitot probe.

### 3.4.4. Example of technique application

An example of the application of modified Pitot tube is shown in Section 4.2.

## 4. Application of multiphase metering for extrapolation of gas/liquid processes in the refinery and petrochemical area

In the petrochemical industry area, many processes are carried out using multiphase reactors since both gas—and liquid—phase reactants are often involved. The reactions being often of catalytic type with a heterogeneous solid supported catalyst, the reactor or absorption column may involve two- or three-phase flow. These very complex flows are not easily predicted by commercial CFD codes and, as a consequence, a precise characterisation of the flow by using an appropriate multiphase metering system is still needed. During the development procedure, when the scale-up of the reactor has to be performed, a global hydrodynamic characterisation is not sufficient and local data are required. Furthermore, at this stage, hard constraints are imposed on measurement: the mock-up equipment to be investigated may be large and the measurement must be handled with real hydrocarbon fluids, under pressure and with the real catalyst support. As a conclusion such metering problems are quite difficult to solve since they must be precise with a good space resolution and must be robust enough to be used in a semi-industrial environment. To illustrate this presentation two types of multiphase reactors have been chosen: fixed bed reactor and slurry bubble column.

### 4.1. Three-phase fixed bed reactors

One of the main problems during the scale-up of such reactors is to optimise the gas/liquid flow distribution across the reactor catalytic bed section. In many cases, the chemical reaction involved is exothermic. In order to optimise the

reaction conversion or selectivity, all the catalytic volume has to be seen by a gas/liquid flow with the same distribution of phases, temperature and pressure. As a matter of fact, an excess of gas in a catalytic zone can for instance accelerate the reaction and so the local heat generation. This zone being, in the same time, not refreshed by enough liquid flow rate, a hot spot can occur, that will dramatically affect reactor performance. The desirable uniform gas/liquid flow distribution is all the more difficult to achieve as the reactor diameter increases. During the development procedure, the flow distribution has therefore to be correctly determined on large size mock-up equipment : typically 40 or 60 cm in diameter.

In a general manner, it is never easy to implement instrumentation inside two-phase flow; but with three-phase gas–liquid–solid conditions, the challenge is even more difficult. The catalytic bed being generally very dense and opaque, no through-the-wall optical method can be used. To better investigate the bed, some local sensors have been developed, such as e.g. optical probes. These probes give interesting information, but the measurement volume being very small, a very large amount of measuring points is necessary to have an idea of the gas–liquid flow distribution over the reactor cross-section. It is thus necessary to develop techniques that determine the flow distribution over the whole reactor section with a good spatial resolution and that are not too intrusive. In this objective, three different techniques have been developed at the French Institute for Petroleum (IFP). The first one is a  $\gamma$ -ray tomographic system to detect the liquid or gas fraction distribution in a reactor slice; the second one is a collecting system that allows to measure the liquid and/or gas flows at the bed outlet, and the third one is an optical probe. The measurement principle and the measuring limitations are fully described in the following sections.

#### 4.1.1. $\gamma$ -ray tomography

The measuring principle of  $\gamma$ -ray tomography has been described in Section 2.2.4. The major problem to overcome with fixed bed reactor is the strong attenuation coming from the solid particles. It is thus necessary to have both a source with rather high activity and several detectors to minimise the measuring time. The new  $\gamma$  tomographic system developed at the IFP is composed of a cesium source of 300 mCi and a series of 32 detectors that are BGO photo-scintillator transducers. The system can be used with reactors of 40 or 60 cm in diameter (Fig. 23). The  $\gamma$ -ray has a fan beam geometry and the whole system is automatically rotated around the reactor. At each angular position a photon attenuation profile is measured. After a complete measurement ( $360^\circ$ ), a map of attenuation can be reconstructed using a classical reconstruction algorithm, filtered back-projection algorithm (Kak & Slaney, 1987). Since the attenuation is directly proportional to the material density, it is possible to determine the liquid or gas holdup by difference between a measurement in dry (or drained) bed configuration and a measure-

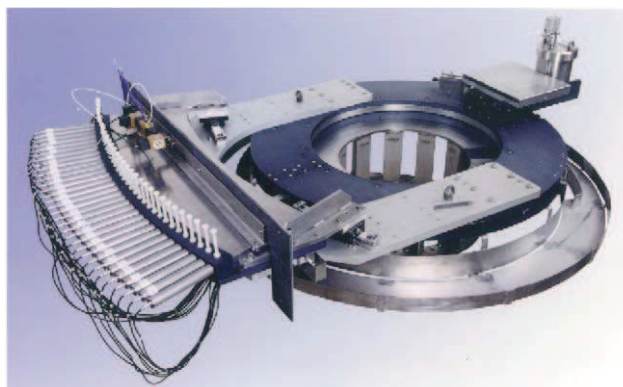


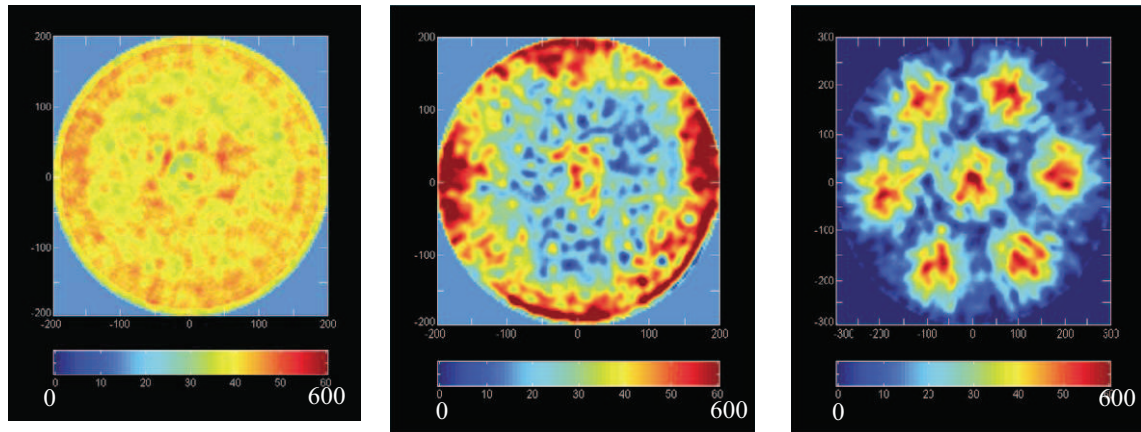
Fig. 23.  $\gamma$ -ray tomographic system for fixed bed reactor.

ment with gas–liquid flow through the catalytic bed. In a similar way, the catalytic bed porosity can be measured by difference between a measurement with dry bed and a measurement with empty column. The reconstructed images have a resolution of  $128 \times 128$  pixels.

The system has been tested under both static and dynamic conditions. Among the different potential measurement errors, the main ones are the statistical error due to random emission of  $\gamma$  photons, the dynamic bias due to gas fraction fluctuations and the reconstruction error. The intrinsic performances of the system have been studied to examine these different potential error sources, and the control parameters, measuring time and scans number, have been optimised (Boyer, Fanget, & Legoupil, 2000). The system is able to measure liquid holdup with an absolute accuracy of 3% for typical measuring time less than 2 h for a column of 60 cm in diameter. Fig. 24 shows examples of measurements of the bed porosity, of the gas fraction in a bubble flow configuration and of the liquid holdup in a trickle flow configuration. Provided the flow remains stable during the measuring time, this system gives the gas or liquid flow distribution with a quite satisfactory spatial resolution. One limitation of the system appears when it is used with porous particles: since it is impossible to discriminate between the liquid remaining inside the particles and that remaining between the particles at rest in drained bed configuration, the liquid holdup measured is only the dynamic liquid holdup.

#### 4.1.2. Device for liquid collection

The second measuring technique has been developed to determine the liquid flow distribution at the catalyst bed outlet. A specific collector tray has been inserted below the trickle bed to sample gas and liquid from 60 sectors of equal surface (Fig. 25). Each gas–liquid stream then flows through a specific gas–liquid separator (Fig. 26). All gas/liquid separating transparent tubes are connected at their top to allow for gas disengagement and to control bottom pressure. Each tube is equipped with restriction valves at the bottom to maintain a constant liquid level. These valves are all calibrated with high precision in order to deduce the liquid



(a) Bed porosity measurement (%) (b) Gas fraction measurement with a liquid flow rate of  $56 \text{ kg/m}^2/\text{s}$  and a gas flow rate of  $0.76 \text{ kg/m}^2/\text{s}$  (c) Liquid fraction measurement with a liquid flow rate of  $1.4 \text{ kg/m}^2/\text{s}$  and a gas flow rate of  $0.39 \text{ kg/m}^2/\text{s}$

Fig. 24. Examples of bed porosity measurement (a); gas fraction measurement (b) and liquid retention measurement (c) inside real catalyst bed of 40 and 60 cm in diameter.

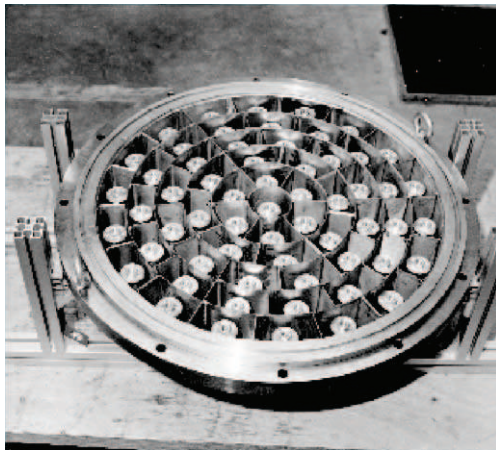


Fig. 25. Collector tray at bed outlet.

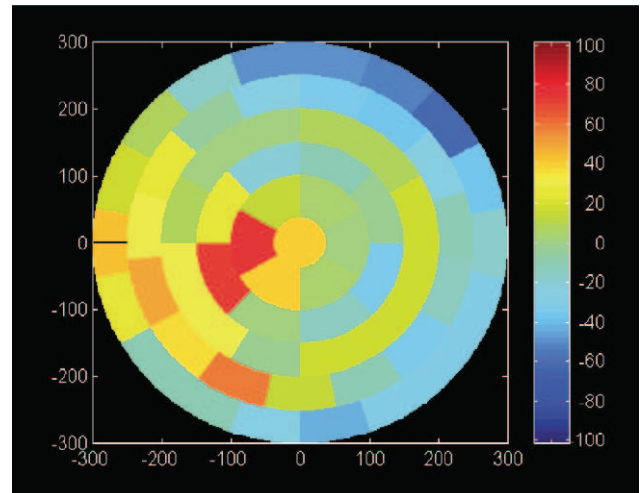


Fig. 27. Example of liquid flow map measured at the bed outlet.



Fig. 26. Gas-liquid separator system associated to the collector tray.

flow rate from the liquid level, the total pressure drop and the valve opening section. Fig. 27 shows a typical flow map obtained with the collecting device with a bad initial liquid distribution. The spatial resolution is limited because of the technical complexity and because the diameter of the collecting lines must be large enough to avoid any disturbing pressure drop. Since this equipment is placed at the bed outlet, when the liquid distribution has to be measured at different levels it is necessary to vary the catalyst bed height inside the column.

#### 4.1.3. Single tip optical probe

Finally, once having studied the gas-liquid distribution, it can be of interest to characterise the gas-liquid interfacial area to have an idea of the mass transfer phenomena

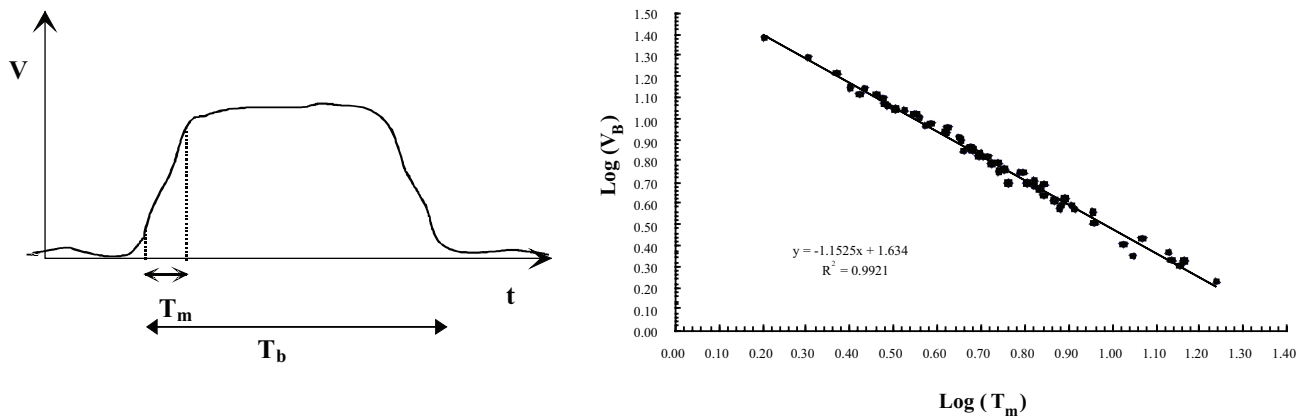


Fig. 28. Measurement principle of the bubble velocity with a single optical probe.

between the phases across the bed. To achieve this objective, a single optical probe technique has been adapted to detect the bubble size inside a trickle bed in bubble flow configuration. The probe is an optical probe as described in the Section 3.1 The measuring principle developed by Cartellier (1992) consists here in correlating the bubble velocity with the drying time of the probe sensing tip when the bubble cross it (see Fig. 28). Once knowing the bubble velocity and the residence time of a bubble on the probe, it is very simple to determine the bubble chord length. This technique needs a calibration procedure for each probe and gas–liquid system used, but only one probe is necessary to determine both velocity and bubble size. As shown in the previous section, it should be noted that this measurement is very sensitive to the angle between bubble direction and probe axis. As a consequence, to be used inside the bed, a protecting grid has to be included around the probe to create a clean measuring volume and control locally the flow. This grid has been tested inside and outside a catalyst bed (Boyer & Cartellier, 1999). The results show that the grid creates locally a small gas channeling, but there is no bubble coalescence across the grid and the bubble velocity and size measured are similar to those measured at the bed outlet. These tests have to be performed under other flow conditions to complete the probe validation but this technique looks very promising.

#### 4.2. Slurry bubble reactor

In this second type of multiphase flow reactor used in the petrochemical area, the reaction takes place in the liquid phase and the gas reactant flows through the liquid phase from bottom to the top of the reactor. The catalyst support is a solid powder dispersed within the liquid phase. In this type of reactor, several hydrodynamic problems have to be solved in order to achieve good conversion performance. The main characteristics to be determined are:

- The liquid-phase agitation: the liquid phase has to be homogeneously mixed, but with moderate liquid local velocities to avoid the catalyst phase deterioration.

- The gas-phase flow configuration: it is necessary to characterise the gas holdup and gas mass flux profiles along the reactor axis and radius.

Concerning the gas flow, the gas holdup and gas velocity profiles are measured using optical probes with a sapphire sensing tip. These probes can be used with solid concentrations up to 10%. For higher solid concentrations, the liquid/solid mixture is simulated by using a liquid of same viscosity and same surface tension. The probe used and the signal analysis have been already described in Section 3.1 of this paper. The typical profiles obtained in a gas–liquid bubble column are described in detail in Schweitzer, Bayle, and Gauthier (2001). These gas holdup profiles are shown to be close to those measured in gas/solid fluidised beds with other optical probes that detect the gas holdup by measuring the light reflected on bubble interface (the sensing tip does not pierce the bubble).

To detect the total average gas and solid holdups, a dynamic measurement of pressure drop is performed at the stop of the unit (Dynamic Gas Disengagement). The gas flow is suddenly interrupted: there is first a disengagement of gas bubbles and then the solid particles settle gently. By measuring the different pressure levels after each step it is possible to determine the gas and solid fraction, knowing the liquid and solid density. Fig. 29 shows an example of pressure measurement during the disengagement procedure. This type of measurement gives precise and robust results but it only provides a global information of the phase fraction over the whole reactor volume and no time-dependant information can be obtained.

In order to determine the liquid-phase agitation, two different kinds of local probes have been used in gas–liquid flow configuration with a liquid of same viscosity and surface tension as the liquid/solid mixture. The first ones are used to measure the overall residence time distribution by local detection of a tracer concentration for determining both axial and radial diffusion coefficients. The second ones are used to measure the local values of liquid velocity.

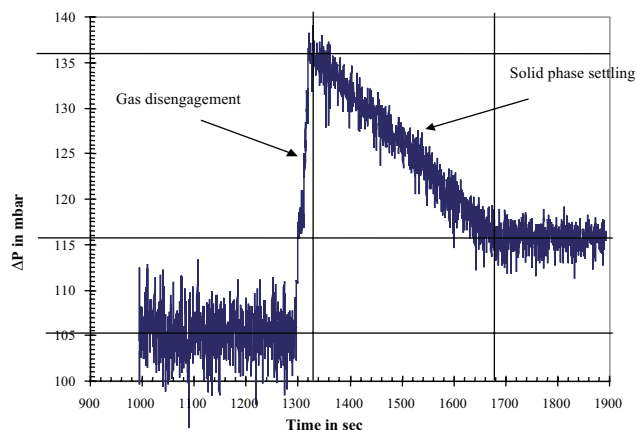


Fig. 29. Pressure drop measurement during the disengagement procedure.

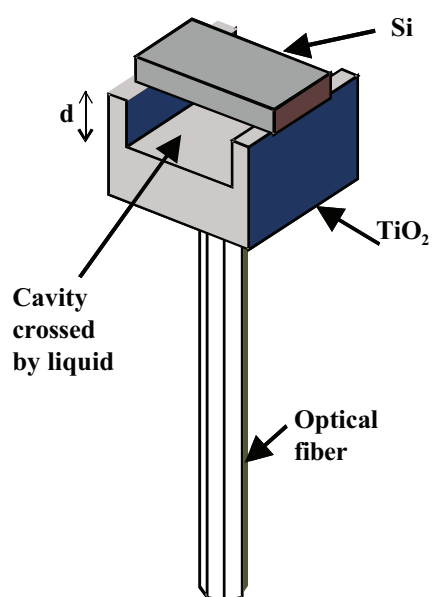


Fig. 30. Geometry of the probe for refractive index measurement.

The axial and radial diffusion coefficients are determined for different values of solid concentration and gas flow rate by performing a residence time analysis at different levels in the slurry bubble column (see Section 2.1.4). The tracer used is a liquid with a refractive index different from that of the liquid used. The tracer is injected into the continuous liquid phase and its concentration is measured by detecting the liquid refractive index with local specific optical probes (Graindorge, Laloux, Girault, Martin, & Lefèvre, 1996). These probes have a very thin sensing tip that includes a cavity crossed by the liquid phase and delimited by two walls (see Fig. 30). A white light beam is sent through an optical fibre to this cavity. The first wall reflects approximately 30% of the light signal and the second wall reflects the other fraction of light that has crossed the liquid phase. By analysing the power spectrum of the resulting light it is possible to detect the wavelength  $\lambda$  corresponding to the

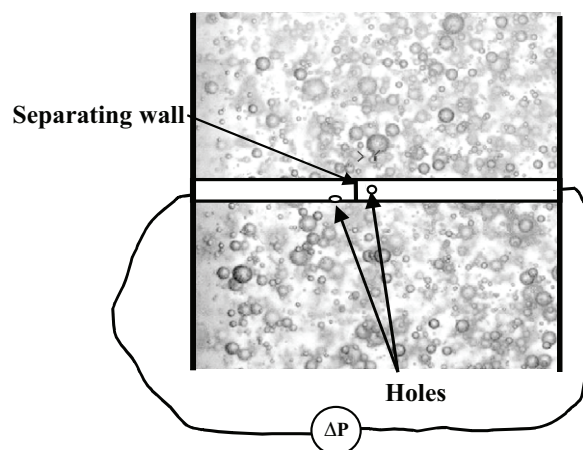


Fig. 31. Modified pitot probe geometry; Warsito et al. (1999).

maximum of interference. For this typical wavelength, there is a direct relation between the cavity width  $d$  and the refractive index  $n$ :

$$n = \frac{3\lambda}{d}. \quad (8)$$

With these probes it is possible to locally detect the tracer concentration at different positions directly inside the reactor without taking account of a sampling line transit time. Since the signal is an optical wave, the response time can be as low as 0.1 ms. This kind of probe can be used with different kinds of liquids (hydrocarbon fluids or aqueous solutions), provided the liquid refractive index ranges from 1.3 to 1.5. In a gas/liquid flow configuration, the probes can be used unless the measuring cavity is totally dried by the gas.

Finally, for the measurement of the local liquid velocity, a modified Pitot probe has been developed. This probe is composed of a single tube separated in two different sections. Two holes are perforated following axis at  $90^\circ$ , one in each tube section (Fig. 31). The two tube sections are connected to a differential pressure drop measurement device. When the liquid flow direction is well known, one hole is oriented face to the flow and the second hole is oriented tangentially to the flow direction. As said in Section 3.4, the liquid velocity can then be deduced from the pressure difference value, once the liquid density is known. When the liquid flow direction is not known, the measuring tube can be rotated and by analysing the pressure drop signals at different angular position it is possible to determine the liquid flow direction and velocity. This type of probe can be used in gas/liquid flow conditions if the liquid phase remains the continuous phase. The problem to overcome is to ensure that no gas bubble is present in the measuring tube by injecting a liquid flow through the pressure lines before each measurement (see Section 3.4). This technique is robust and simple to implement but the measuring tube remains intrusive and must be quite rigid to ensure that the pressure measurements are not perturbed by the tube fluctuations. This modified Pavlov

tube has been used by Hills (1974) and by Vial (2000) in academia, but seldom under industrial conditions.

## 5. Conclusion

Multiphase flows are very complex because of the diversity in nature of the different possible phases and of the different possible flow regimes. Their experimental investigation is therefore not easy and the most recent non-invasive local techniques (Particle Image Velocimetry for instance) are useless in most cases. Multiphase flow analysis requires dedicated measuring methods to get local or global data.

This paper offers a review of measuring techniques available to characterise multiphase systems such as the gas-liquid or gas-liquid-solid reactors that are heavily encountered in process engineering area. The very large variety of existing techniques puts in evidence the intense worldwide research activity devoted to develop appropriate multiphase flow instrumentation.

For each type of multiphase flow encountered, there is often not only one technique to be recommended, as shown by the examples of application reported in Section 3. The final choice must take into account the spatial and time resolution required, the measuring constraints (presence of solid, of hydrocarbon fluids), the expected range of measuring values (high or low holdups) and the disturbance and inaccuracy allowed. Several techniques may be simultaneously derived to get complementary data.

## References

- Bakshi, B. R., Zhong, H., Jiang, P., & Fan, L-S. (1995). Analysis of flow in gas-liquid bubble columns using multi-resolution methods. *Transactions of the Institution of Chemical Engineers, A: Chemical Engineering Research and Design*, 73, 608–614.
- Barrau, E., Rivière, N., Poupot, C., & Cartellier, A. (1999). Single and double optical probes in air-water two-phase flows: Real time signal processing and sensor performance. *International Journal of Multiphase Flow*, 25, 229–256.
- Bauchhage, K. (1996). Gleichzeitige Erfassung von Partikelmerkmalen und Eigenschaften mehrphasiger Strömungen mit Hilfe der Phasen-Doppler-Anemometrie. *Chemie-Ingenieur-Technik*, 68, 253–266.
- Becker, S., De Bie, H., & Sweeney, J. (2000). Study on the flow structure in an aerated flat apparatus using laser Doppler anemometry. *Chemical Engineering and Technology*, 23, 222–226.
- Begovich, J. M., & Watson, J. S. (1978). An electroconductivity method for the measurement of axial variation of holdups in three-phase fluidized beds. *American Institute of Chemical Engineers Journal*, 24, 351–354.
- Beinhauer, R. (1971). *Dynamische Messungen des relativen Gasgehalts in Blasensäulen mittels Absorption von Röntgenstrahlen*. Dissertation TU Berlin; cited by Deckwer (1985).
- Bendjaballah, N., Dhaouadi, H., Poncin, S., Midoux, N., Hornut, J. M., & Wild, G. (1999). Hydrodynamics and flow regimes in external loop airlift reactors. *Chemical Engineering Science*, 54, 5211–5221.
- Bendjaballah-Lalaoui, N. (2000). *Hydrodynamique globale et locale dans un réacteur à gazosiphon à recirculation externe*. Thèse de doctorat, Institut National Polytechnique de Lorraine, Nancy, France.
- Bensler, H.P. (1990). *Détermination de l'aire interfaciale, du taux de vide et du diamètre moyen de Sauter dans un écoulement à bulles à partir de l'atténuation d'un faisceau d'ultrasons*. Thèse de doctorat, Institut National Polytechnique de Grenoble, France.
- Bentifraouine, C. (1997). *Hydrodynamique globale, locale et transfert de matière dans un réacteur airlift à boucle externe*. Thèse de doctorat, Institut National Polytechnique de Toulouse, France.
- Bigot, V., Guyot, L., Bataille, D., & Roustan, M. (1990). Possibilités d'utilisation de deux techniques métrologiques, capteurs de pression et fibres optiques, pour caractériser l'hydrodynamique d'un lit fluidisé triphasique. In A. Storck, & G. Wild (Eds.), *Récents Progrès en Génie des Procédés*, Vol. 10 (pp. 143–149). Technique et Documentation. Paris: Lavoisier.
- Blet, V., Berne, P., Chaussy, C., Perrin, S., & Schweich, D. (1999). Characterization of a packed column using radioactive tracers. *Chemical Engineering Science*, 54, 91–101.
- Bouillard, J., Alban, B., Jacques, P., & Xuereb, C. (2001). Liquid flow velocity measurements in stirred tanks by ultra-sound Doppler velocimetry. *Chemical Engineering Science*, 56, 747–754.
- Boyd, J. W. R., & Varley, J. (1998). Sound measurement as a means of gas-bubble sizing in aerated agitated tanks. *American Institute of Chemical Engineers Journal*, 44, 1731–1739.
- Boyer, C. (1996). *Etude d'un procédé de mesure des débits d'un écoulement triphasique type caulhuile/gaz*. Thèse de doctorat, Institut National Polytechnique de Grenoble, France.
- Boyer, C., & Cartellier, A. (1999). Bubble velocity and size estimation using a single optical probe in a gas/liquid flow across a fixed bed reactor. *Récents Progrès en Génie des Procédés*, 13(69), 379–386.
- Boyer, C., Fanget, B., & Legoupil, S. (2000). Development of a new Gamma-Ray Tomographic system to investigate two-phase gas/liquid flows in trickle bed reactor of large diameter. *CHISA'2000, Proceedings Paper no. 588*, Prague.
- Briens, L. A., Briens, C. L., Hay, J., Hudson, C., & Margaritis, A. (1997a). Hurst's analysis to detect minimum fluidization and gas maldistribution in fluidized beds. *American Institute of Chemical Engineers Journal*, 43, 1904–1908.
- Briens, L. A., Briens, C. L., Margaritis, A., & Hay, J. (1997b). Minimum liquid fluidization velocity in gas-liquid-solid fluidized beds. *American Institute of Chemical Engineers Journal*, 43, 1180–1189.
- Briens, C. L., Margaritis, A., & Wild, G. (1995). A new stochastic model and measurement errors in residence time distributions of multiphase reactors. *Chemical Engineering Science*, 50, 279–287.
- Bröder, D., Lain, S., & Sommerfeld, M. (2000). Experimental studies of the hydrodynamics in a bubble column. In R. Köpsel, & P. Kuchling (Eds.), *Fifth German-Japanese symposium bubble columns* (pp. 125–130). Medienzentrum der Bergakademie Freiberg: VDI, ISBN 3-86012-109-X 2000.
- Bröring, S., Fischer, J., Korte, T., Sollinger, S., & Lübbert, A. (1991). Flow structure of the dispersed gasphase in real multiphase chemical reactors investigated by a new ultrasound-Doppler technique. *Canadian Journal of Chemical Engineering*, 69, 1247–1256.
- Brück, F. J., & Hektor, K. (1984). Einsatz der Vierpunkt-Leitfähigkeitsmikrosonde im Dreiphasen-Fließbett. *Chemie-Ingenieur-Technik*, 56, 920–922.
- Brunns, H. H. (1995). *Hot wire anemometry. Principles and signal analysis*. New York: Oxford University Press Inc.
- Buchholz, R., Tseptonides, J., Steinemann, J., & Onken, U. (1983). Influence of gas distribution on interfacial area and mass transfer in bubble columns. *German Chemical Engineering*, 6, 105–113.
- Buchholz, R., Zakrzewsky, W., & Schügerl, K. (1981). Techniques for determining the properties of bubbles in bubble columns. *International Chemical Engineering*, 21, 180–187.
- Buffham, B. A., & Mason, G. (1993). Hold-up and dispersion: Tracer residence times, moments and inventory measurements. *Chemical Engineering Science*, 48, 3879–3887.

- Burgess, J. M., & Calderbank, P. H. (1975). The measurement of bubble parameters in two-phase dispersions II. The structure of sieve tray froths. *Chemical Engineering Science*, 30, 1107–1121.
- Calderbank, P. H. (1958). Physical rate processes in industrial fermenters. Part I: The interfacial area in gas/liquid contacting with mechanical agitation. *Transactions of the Institution of Chemical Engineers*, 36, 443–463.
- Callaghan, P. T. (1991). *Principles of nuclear magnetic resonance microscopy*. New York: Oxford University Press.
- Camarasa, E., Vial, C., Poncin, S., Wild, G., Midoux, N., & Bouillard, J. (1999). Influence of coalescence behaviour of the liquid and of gas sparging on hydrodynamics and bubble characteristics in a bubble column. *Chemical Engineering and Processing*, 38, 329–344.
- Cartellier, A. (1992). Simultaneous void fraction measurement, bubble velocity, and size estimate using a single optical probe in gas–liquid two-phase flows. *Review of Scientific Instruments*, 63, 5442–5453.
- Cartellier, A., & Achard, J.-L. (1991). Local detection probes in fluid–fluid two-phase flows. *Review of Scientific Instruments*, 62(2), 279–303.
- Cartellier, A., Poupot, C., Chambérod, E., & Barrau, E. (1996). Sondes optiques: Innovations sur un capteur classique. *La Houille Blanche*, 112, 120–128.
- Cassanello, M., Larachi, F., Marie, M. N., Guy, C., & Chaouki, J. (1995). Experimental characterization of the solid phase chaotic dynamics in three-phase fluidization. *Industrial and Engineering Chemistry Research*, 34, 2971–2980.
- Chabot, J., & De Lasa, H. I. (1993). Gas holdups and bubble characteristics in a bubble column operated at high temperature. *Industrial and Engineering Chemistry Research*, 32, 2595–2601.
- Chabot, J., Farag, H., & De Lasa, H. (1998). Fluid dynamics of bubble columns at elevated temperature modelling and investigation with refractive fiber optic sensor. *The Chemical Engineering Journal*, 70, 105–113.
- Chabot, J., Lee, S. L. P., Soria, A., & De Lasa, H. I. (1992). Interaction between bubbles and fiber optic probes in a bubble column. *Canadian Journal of Chemical Engineering*, 70, 61–68.
- Chaouki, J., Larachi, F., & Dudukovic, M. P. (1997). Noninvasive tomographic and velocimetric monitoring of multiphase flows. *Industrial and Engineering Chemistry Research*, 36, 4476–4503.
- Chen, J., Kemoun, A., Al-Dahhan, M. H., Dudukovic, M. P., Lee, D. J., & Fan, L.-S. (1999). Comparative hydrodynamics study in bubble columns using computer-automated radioactive particle tracking (CARPT)/computed tomography (CT) and particle image velocimetry (PIV). *Chemical Engineering Science*, 54, 2199–2207.
- Chen, Z., Zheng, C., Feng, Y., & Hofmann, H. (1998). Local bubble behavior in three-phase fluidized beds. *Canadian Journal of Chemical Engineering*, 76, 315–318.
- Cho, S. H., & Becker, H. A. (1985). Response of static pressure probes in turbulent streams. *Experiments in fluids*, 3, 93–102.
- Choi, K. H., & Lee, W. K. (1990). Comparison of probe methods for measurement of bubble properties. *Chemical Engineering Communications*, 91, 35–47.
- Chue, S. H. (1975). Pressure probes for fluid measurements. In D. Kuchemann (Ed.), *Progress in aerospace sciences*, Vol. 16 (pp. 147–223).
- Clark, N. N., & Turton, R. (1988). Chord length distributions related to bubble size distributions in multiphase flows. *International Journal of Multiphase Flow*, 14, 413–424.
- Daly, J. G., Patel, S. A., & Bukur, D. B. (1992). Measurement of gas holdups and Sauter mean bubble diameters in bubble column reactors by dynamic gas disengagement method. *Chemical Engineering Science*, 47, 3647–3654.
- Deckwer, W.-D. (1985). *Reaktionstechnik in Blasensulenä*. Frankfurt, Aarau: Salle+Sauerländer.
- Delnoij, E., Kuipers, J. A. M., van Swaaij, W. P. M., & Westerweel, J. (2000). Measurement of gas–liquid two-phase flow in bubble columns using ensemble correlation PIV. *Chemical Engineering Science*, 55, 3385–3395.
- Dhaouadi, H., Poncin, S., Hornut, J.-M., Wild, G., Oinas, P., & Korpajarvi, J. (1997). Mass transfer in an external loop airlift reactor: Experiments and modeling. *Chemical Engineering Science*, 52, 3909–3917.
- Dias, S. G., França, F. A., & Rosa, E. S. (2000). Statistical method to calculate local interfacial variables in two-phase bubbly flows using intrusive crossing probes. *International Journal of Multiphase Flow*, 26, 1797–1830.
- Drahos, J., Bradka, F., & Puncochar, M. (1992). Fractal behaviour of pressure fluctuations in a bubble column. *Chemical Engineering Science*, 47, 4069–4075.
- Drahos, J., & Cermak, J. (1989). Diagnostics of gas–liquid flow patterns in chemical engineering systems. *Chemical Engineering and Processing*, 26, 147–164.
- Drahos, J., Zahradnik, J., Puncochar, M., Fialova, M., & Bradka, F. (1991). Effect of operating conditions of the characteristics of pressure fluctuations in a bubble column. *Chemical Engineering and Processing*, 29, 107–115.
- Dudukovic, M. P., Devanathan, N., & Holub, R. (1991). Multiphase reactors: Models and experimental verification. *Revue de l'Institut Français du Pétrole*, 46, 439–465.
- Euzen, J.-P., & Fortin, Y. (1987). Partikelbewegung in einem Dreiphasenfließbett. *Chemie-Ingenieur-Technik*, 59, 416–419.
- Fan, L. S., & Tsuchiya, K. (1990). *Bubble wake dynamics in liquids and liquid-solid suspensions*. Stoneham, MA, USA: Butterworths-Heinemann Series in Chemical Engineering.
- Farrar, B. (1988). *Hot-film anemometry in dispersed oil–water flows*. Ph.D. thesis, Department of Mechanical and Manufacturing Engineering, University of Bradford, UK.
- Farrar, B., Samways, A. L., Ali, J., & Bruun, H. H. (1995). A computer based hot-film technique for two-phase flow measurements. *Measurements in Science and Technology*, 6, 1528–1537.
- Fingerson, L. M., & Freymouth, P. (1983). Thermal anemometers. In R. J. Goldstein (Ed.), *Fluid mechanics measurements* (pp. 99–154). Washington: Hemisphere.
- Fischer, J., Bröring, S., & Lübbert, A. (1992). Gas-phase properties in stirred tank bioreactors. *Chemical Engineering Technology*, 15, 390–394.
- Flaschel, E., Metzdorf, C., & Renken, A. (1987). Methode zur Messung der axialen Vermischung des Feststoffs in Flüssigkeit/Feststoff-Wirbelschichten. *Chemie-Ingenieur-Technik*, 59, 494–496.
- Fortin, Y. (1984). *Réacteurs à lit fluidisé triphasique: caractéristiques hydrodynamiques et mélange des particules solides*. Thèse de docteur-ingénieur, Université de Paris VI, ENSPM, Solaize, France.
- Fournier, T., & Jeandey, C. (1993). Optimization of an experimental setup for void fraction determination by the X-ray attenuation technique. In J.M. Delhaye & G. Cagnet (Eds.), *Measuring techniques in gas–liquid two-phase flows* (pp. 199–228). Berlin, Heidelberg, New York, Tokyo: Springer.
- Fröhlich, S., Lotz, M., Larson, B., Lübbert, A., Schügerl, K., & Seekamp, M. (1991). Characterization of a pilot plant airlift tower loop reactor: III. Evaluation of local properties of the dispersed gas phase during yeast cultivation and in model media. *Biotechnology and Bioengineering*, 38, 56–64.
- Froystein, T. (1997). Flow imaging by gamma-ray Tomography: Data processing and reconstruction techniques. *Frontiers in Industrial Process Tomography II*, Delft, April 8–12, 1997.
- Funfschilling, D., & Li, H.-Z. (2001). Flow of non-Newtonian fluids around bubbles: PIV measurements and birefringence visualisation. *Chemical Engineering Science*, 56, 1137–1141.
- García Ochoa, J., Khalifet, R., Poncin, S., & Wild, G. (1997). Hydrodynamics and Mass Transfer in a suspended solid bubble column with polydispersed high density particles. *Chemical Engineering Science*, 52, 3827–3834.
- Gladden, L. F. (1994). Nuclear magnetic resonance in chemical engineering: Principles and applications. *Chemical Engineering Science*, 49, 3339–3408.

- Glasgow, L. A., Erickson, L. E., Lee, C. H., & Patel, S. A. (1984). Wall pressure fluctuations and bubble size distributions at several positions in an airlift fermentor. *Chemical Engineering Communications*, 29, 311–336.
- Glasgow, L. A., Hua, J., Yiin, T. Y., & Erickson, L. E. (1992). Acoustic studies of interfacial effects in airlift reactors. *Chemical Engineering Communications*, 113, 155–181.
- Graindorge, Ph., Laloux, B., Girault, M., Martin, Ph., & Lefèvre, H. C. (1996). Metricor 2000: A multiparameter fiber-optic sensor instrument. *Fiber optic and laser sensor XIV*, 7–9 August 1996, Denver, CO.
- Groen, J. S., Mudde, R. F., & van den Akker, H. E. A. (1995). Time dependant behaviour of the flow in a bubble column. *Transactions of the Institution of Chemical Engineers, A: Chemical Engineering Research and Design*, 73, 615–620.
- Gupta, P., Al-Dahhan, M. H., Dudukovic, M. P., & Mills, P. L. (2000). A novel signal filtering methodology for obtaining liquid phase tracer responses from conductivity probes. *Flow Measurement and Instrumentation*, 11, 123–131.
- Haario, H. (1994). *MODEST user's guide*. Helsinki, Finland: Profmath.
- Heindel, T. J. (2000). Gas flow regime changes in a bubble column filled with a fibre suspension. *Canadian Journal of Chemical Engineering*, 78, 1017–1022.
- Hills, J. H. (1974). Radial non-uniformity of velocity and voidage in a bubble column. *Transactions of the Institution of Chemical Engineers*, 52, 1–7.
- Hogsett, S., & Ishii, M. (1997). Local two-phase flow measurements using sensor techniques. *Nuclear Engineering and Design*, 175, 15–24.
- Jakobsen, H. A., Svendsen, H. F., & Hjarbo, K. W. (1992). On the prediction of local flow structures in internal loop and bubble column reactors using a two-fluid model. *Computers & Chemical Engineering*, 175, 5531–5536.
- Johnsson, F., Zijerveld, R. C., Schouten, J. C., van den Bleek, & C. M., & Leckner, B. (2000). Characterization of fluidization regimes by time-series analysis of pressure fluctuations. *International Journal of Multiphase Flow*, 26, 663–715.
- Jones, O. C., & Delhaye, & J. M. (1976). Transient and statistical measurement techniques for two-phase flows. *International Journal of Multiphase Flow*, 3, 89.
- Jones, O. C., & Zuber, N. (1978). Use of a cylindrical hot-film anemometer for measurement of two-phase void and volume flux profiles in a narrow rectangular channel. *American Institute of Chemical Engineers Symposium Series*, 74(174), 191–204.
- Joseph, S., & Shah, Y. T. (1986). Errors caused by tracer solubility in the measurement of gas phase axial dispersion. *Canadian Journal of Chemical Engineering*, 64, 380–386.
- Joshi, J. B. (2001). Computational flow modelling and design of bubble column reactors. *Chemical Engineering Science*, 56, 5893–5933.
- Joshi, J. B., Patil, T. A., Ranade, V. V., & Shah, Y. T. (1990). Measurement of hydrodynamic parameters in multiphase sparged reactors. *Reviews in Chemical Engineering*, 6(2–3), 73–227.
- Kak, A. C., & Slaney, M. (1987). *Computerized tomographic imaging*. New York: IEEE Press.
- Kamp, A. M. Colin, C., & Fabre, J. (1995). Techniques de mesure par sonde optique double en écoulement diphasique à bulles. *Cert Onera, Colloque de Mécanique des Fluides Expérimentale*, Toulouse, France, 11–12 May, 1995.
- Kang, Y., Cho, Y. J., Woo, K. J., Kim, K. I., & Kim, S. D. (2000). Bubble properties and pressure fluctuations in pressurized bubble columns. *Chemical Engineering Science*, 55, 411–419.
- Kasireddy, V. K., & Al Taweel, A. M. (1990). An improved light attenuation technique for measuring large interfacial areas. *Canadian Journal of Chemical Engineering*, 68, 690–693.
- Kataoka, I., Ishii, M., & Serizawa, A. (1986). Local formulation and measurements of interfacial area concentration in two-phase flow. *International Journal of Multiphase Flow*, 12, 505–529.
- Kikuchi, R., Tsutsumi, A., & Yoshida, K. (1997). Stochastic analysis of bubble and particle motions in a 2-D three-phase reactor. *Journal of Chemical Engineering of Japan*, 30, 202–209.
- Kluytmans, J. H. J., van Wachem, B. G. M., Kuster, B. F. M., Schouten, J. C. (2001). Gas hold-up in a slurry bubble column: Influence of electrolyte and carbon particles. *Industrial and Engineering Chemistry Research*, submitted for publication.
- Kolb, W. B., Melli, T. R., de Santos, J. M., & Scriven, L. E. (1990). Cocurrent downflow in packed beds. Flow regimes and their acoustic signatures. *Industrial and Engineering Chemistry Research*, 29, 2380–2389.
- Kumar, S. B., Moslemian, D., & Dudukovic, M. P. (1995). A gamma-ray tomographic scanner for imaging voidage distribution in two-phase flow systems. *Flow Measurement Instrumentation*, 6, 61–73.
- Lage, P. L. C., & Espósito, R. O. (1999). Experimental determination of bubble size distributions in bubble columns: Prediction of mean bubble diameter and gas hold up. *Powder Technology*, 101, 142–150.
- Lance, M., & Bataille, J. (1983). Turbulence in the liquid phase of a bubbly air–water flow. *Advances in two-phase flow and heat transfer*, 1, 403–427. NATO Specialist Meeting, NATO Advances Science Institute Series, West Germany.
- Lara Márquez, A. (1992). *Etude du transfert de matière gaz-liquide dans les réacteurs à lit fixe avec écoulement à cocourant ascendant de gaz et de liquide*. Thèse de doctorat, Institut National Polytechnique de Lorraine, Nancy, France.
- Larachi, F., Chaouki, J., & Kennedy, G. (1995). Three dimensional mapping of solids flow fields in multiphase reactors with RPT. *American Institute of Chemical Engineers Journal*, 41, 439–443.
- Larachi, F., Laurent, A., Wild, G., & Midoux, N. (1991). Some experimental liquid saturation results in fixed-bed reactors operated under elevated pressure in cocurrent upflow and downflow of the gas and the liquid. *Industrial and Engineering Chemistry Research*, 30, 2404–2410.
- Latifi, M. A., Naderifar, A., & Midoux, N. (1994a). Stochastic analysis of the local velocity gradient in a trickle-bed reactor. *Chemical Engineering Science*, 49, 5281–5289.
- Latifi, M. A., Naderifar, A., Midoux, N., & Le Méhauté, A. (1994b). Fractal behaviour of local liquid-solid mass transfer fluctuations at the wall of a trickle-bed reactor. *Chemical Engineering Science*, 49, 3823–3829.
- Latifi, M. A., Rode, S., Midoux, N., & Storck, A. (1992). The use of microelectrodes for the determination of flow regimes in a trickle-bed reactor. *Chemical Engineering Science*, 47, 1955–1961.
- Leclerc, J.-P., Claudel, S., Lintz, H.-G., Potier, O., & Antoine, B. (2000). Theoretical interpretation of residence-time distribution measurements in industrial processes. *Oil and Gas Science and Technology—Revue de l'Institut Français du Pétrole*, 55, 159–169.
- Lee, S. L. P., & De Lasa, H. I. (1987). Phase holdups in three-phase fluidized beds. *American Institute of Chemical Engineers Journal*, 33, 1359–1370.
- Lee, D. J., Luo, X., & Fan, L.-S. (1999). Gas disengagement technique in a slurry bubble column operated in the coalesced bubble regime. *Chemical Engineering Science*, 54, 2227–2236.
- Lesage, F. (2000). *Modélisation et expérimentation des transferts de matière et de quantité de mouvement dans les réacteurs à lit fixe*. Thèse de doctorat, Institut National Polytechnique de Lorraine, Nancy, France.
- Letzel, H. M., Schouten, J. C., Krishna, R., & van den Bleek, C. M. (1997). Characterisation of regimes and regime transitions in bubble columns by chaos analysis of pressure signals. *Chemical Engineering Science*, 52, 4447–4459.
- Levenspiel, O. (1999). *Chemical reaction engineering* (3rd ed.). New York: Wiley.
- Ligrani, P. M., Singer, B. A., & Baun, L. R. (1989). Miniature five-hole pressure probe for measurement of three mean velocity components in low speed flow. *Journal of Physics E: Scientific Instruments*, 22, 868–876.
- Lin, T.-J., Juang, R.-C., Chen, Y.-C., & Chen, C.-C. (2001). Predictions of flow transitions in a bubble column by chaotic time series analysis

- of pressure fluctuation signals. *Chemical Engineering Science*, 56, 1057–1065.
- Lin, T.-J., Tsuchiya, K., & Fan, L.-S. (1998). Bubble flow characteristics in bubble columns at elevated pressure and temperature. *American Institute of Chemical Engineers Journal*, 44, 545–560.
- Liu, T. J. (1993). Bubble size and entrance length effects on void development in a vertical channel. *International Journal of Multiphase Flow*, 19, 99–113.
- Liu, W., Clark, N. N., & Karamavruc, A. I. (1998). Relationship between bubble size distributions and chord-length distribution in heterogeneously bubbling systems. *Chemical Engineering Science*, 53(6), 1267–1276.
- Lübbert, A. (1991). Characterization of bioreactors. In H.J. Rehm, G. Reed, A. Pühler, & P. Stadler (Eds.), *Biotechnology* (2nd ed.). Vol. 4. (pp. 107–148). Weinheim, New York: Verlag Chemie.
- Luewisuthichat, W., Tsutsumi, A., & Yoshida, K. (1995). Fractal analysis of particle trajectories in three-phase systems. *Transactions of the Institution of Chemical Engineers, A: Chemical Engineering Research and Design*, 73, 222–227.
- Luewisuthichat, W., Tsutsumi, A., & Yoshida, K. (1996). Deterministic chaos analysis of particle dynamics in three-phase systems. *Journal of Chemical Engineering of Japan*, 29, 675–682.
- Magaud, F. (1999). *Contribution expérimentale sur l'étude d'écoulements à bulles de type contacteur gaz-liquide*. Thèse de doctorat, Institut National Polytechnique de Lorraine, Nancy, France.
- Magaud, F., Souhar, M., Wild, G., & Boisson, N. (2001). Experimental study of bubble columns hydrodynamics. *Chemical Engineering Science*, 56, 4597–4607.
- Mann, R., Dickin, F. J., Wang, M., Dyakowski, T., Williams, R. A., Edwards, R. B., Forrest, A. E., & Holden, P. J. (1997). Application of electrical resistance tomography to interrogate mixing processes at plant scale. *Chemical Engineering Science*, 52, 2087–2097.
- Marcandelli, C., Lamine, A. S., Bernard, J. R., & Wild, G. (2000). Liquid distribution in trickle-bed reactor. *Oil and Gas Science and Technology*, 55(4), 407–415.
- Matsui, G. (1984). Identification of flow regimes in vertical gas–liquid two-phase flow using differential pressure fluctuations. *International Journal of Multiphase Flow*, 10, 711–720.
- Maucci, E., Briens, C. L., Martinuzzi, R. J., & Wild, G. (1999). Detection and characterization of piston flow regime in three-phase fluidized beds. *Powder Technology*, 103, 243–259.
- Mawlana, A., Huang, H., Wilhelm, A. M., & Delmas, H. (1992). Transferable tracer analysis for multiphase reactor. *Chemical Engineering Communications*, 115, 67–82.
- Menzel, T., In Der Weide, T., Staudacher, O., Wein, O., & Onken, U. (1990). Reynolds shear stress for modeling of bubble column reactors. *Industrial and Engineering Chemistry Research*, 29, 988–994.
- Mitchell, J. E., & Hanratty, T. J. (1966). A study of turbulence at a wall using an electrochemical wall shear–stress meter. *Journal of Fluid Mechanics*, 26, 199–221.
- Miyahara, T., Hamaguchi, M., Sukeda, Y., & Takahashi, T. (1986). Size of bubbles and liquid circulation in a bubble column with a draught tube and a sieve plate. *Canadian Journal of Chemical Engineering*, 64, 718–725.
- Moujaes, S. F. (1990). Testing a spherical dual-tipped optical fiber probe for local measurements of void fraction and gas velocity in two-phase flows. *Canadian Journal of Chemical Engineering*, 68, 504–510.
- Moujaes, S., & Dougall, R. S. (1987). Experimental investigation of cocurrent two-phase flow in a vertical rectangular channel. *Canadian Journal of Chemical Engineering*, 65, 705–715.
- Müdde, R. F., Groen, J. S., & van den Akker, H. E. A. (1997). Liquid velocity field in a bubble column: LDA experiments. *Chemical Engineering Science*, 52, 4217–4224.
- Müdde, R. F., Groen, J. S., & van den Akker, H. E. A. (1998). Application of LDA to bubbly flows. *Nuclear Engineering and Design*, 184, 329–338.
- Murai, Y., Song, X. Q., Takagi, T., Ishikawa, M., Yamamoto, F., & Ohta, J. (2000). Inverse energy cascade structure of turbulence in a bubbly flow. PIV measurement and results *Japanese Society of Mechanical Engineers International Journal Series B, Fluids and Thermal Engineering*, 43(2), 188–196.
- Naderifar, A. (1995). *Etude expérimentale locale et globale du transfert de matière liquidelsolide à la paroi d'un réacteur à lit fixe*. Thèse de doctorat, Institut National Polytechnique de Lorraine, Nancy, France.
- Nakoryakov, V. E., Kashinsky, O. N., & Kozenko, B. K. (1984). Electrochemical method for measuring turbulent characteristics of gas–liquid flows. In J.M. Delhaye, & G. Cagnet (Eds.), *Measuring techniques in gas–liquid two-phase flows* (pp. 695–721). Berlin, Heidelberg, New York, Tokyo: Springer.
- Nicol, R. S., & Davidson, J. F. (1988). Gas holdup in circulating bubble columns. *Transactions of the Institution of Chemical Engineers, A: Chemical Engineering Research and Design*, 68, 152–158.
- Northrup, M. A., Kulp, T. S., Angel, S. M., & Pinder, G. F. (1993). Direct measurement of interstitial velocity field variations in a porous medium using fluorescent-particle image velocimetry. *Chemical Engineering Science*, 48, 13–21.
- Pannek, S., Pauli, J., & Onken, U. (1994). Determination of local hydrodynamic parameters in bubble columns by the electrodiffusion method with oxygen as a depolarizer. *Journal of Applied Electrochemistry*, 24, 666–669.
- Pant, H. J., Saroha, A. K., & Nigam, K. D. P. (2000). Measurement of liquid holdup and axial dispersion in trickle bed reactors using radiotracer technique. *Nukleonika*, 45(4), 235–241.
- Pauli, J., Menzel, T., & Onken, U. (1989). Diffusional specific shear-rate measurements in gas–liquid two-phase flow. *Chemical Engineering Technology*, 12, 374–378.
- Pauli, J., Onken, U., & Sobolík, V. (1991). Electrodiffusional direction-specific probe for measuring local velocity of aerated aqueous systems. *Journal of Applied Electrochemistry*, 21, 1073–1076.
- Peterson, D. A., Tankin, R. S., & Bankoff, S. G. (1984). Holographic measurements of bubble size and velocity in three-phase systems. In J.M. Delhaye & G. Cagnet (Eds.), *Measuring techniques in gas–liquid two-phase flows* (pp. 1–21). Berlin, Heidelberg, New York, Tokyo: Springer.
- Prasser, H.-M., Böttger, A., & Zschau, J. (1998). A new electrode-mesh tomograph for gas–liquid flows. *Flow Measurement and Instrumentation*, 9, 111–119.
- Purwasasmita, M. (1985). *Contribution à l'étude des réacteurs à lit fixe fonctionnant à co-courant vers le bas à fortes vitesses du gaz et du liquide*. Thèse de doctorat, Institut National Polytechnique de Lorraine, Nancy, France.
- Reese, J., Mudde, R. F., Lee, D. J., & Fan, L. -S. (1996). Analysis of multiphase systems through particle image velocimetry. *American Institute of Chemical Engineers Symposium Series*, 92(310), 161–167.
- Reinecke, N. (1996). *Kapazitive Tomographie für transiente Mehrphasenströmungen*. Dissertation, Fakultät für Maschinenwesen, Universität Hannover, Germany.
- Reinecke, N., & Mewes, D. (1997). Investigation of the two-phase flow in trickle-bed reactors using capacitance tomography. *Chemical Engineering Science*, 52, 2111–2127.
- Reinecke, N., Petritsch, G., Schmitz, D., & Mewes, D. (1998). Tomographic measurement techniques—Visualisation of multiphase flow. *Chemical Engineering Technology*, 21, 7–18.
- Reiss, L. P., & Hanratty, T. J. (1963). An experimental study of the unsteady nature of the viscous sublayer. *A.I.Ch.E. Journal*, 9, 154–160.
- Resch, F. J., & Leutheusser, H. J. (1972). Reynolds stress measurements in hydraulic jumps. *Journal of Hydraulic Research*, 10(4), 409–430.
- Resch, F. J., Leutheusser, H. J., & Alemu, S. (1974). Bubbly two-phase flow in hydraulic jump. *Proceedings of the American society of civil engineers, Journal of Hydraulic Division*, 100(HY1), 137–149.

- Revankar, S. T., & Ishii, M. (1992). Local interfacial area measurement in bubbly flow. *International Journal of Heat and Mass Transfer*, 25, 913–925.
- Rode, S., Midoux, N., Latifi, M. A., & Storck, A. (1994). Hydrodynamics and liquid–solid mass transfer mechanisms in packed beds operating in cocurrent gas–liquid downflow: An experimental study using electrochemical shear rate sensors. *Chemical Engineering Science*, 49, 1383–1401.
- Roig, V., Larrieu, N., & Suzanne, C. (1995). Turbulent length scales in bubbly mixing layer. *International symposium on two-phase flow modelling and experimentation*, Rome.
- Roig, V., Suzanne, C., & Masbernat, L. (1998). Experimental investigation of a turbulent bubbly mixing layer. *International Journal of Multiphase Flow*, 24, 35–54.
- Roizard, C., Poncin, S., Lapique, F., Py, X., & Midoux, N. (1999). Behavior of fine particles in the vicinity of a gas bubble in a stagnant and a moving fluid. *Chemical Engineering Science*, 54, 2317–2323.
- Rüffer, H. M., Bröring, S., & Schügerl, K. (1995). Fluid dynamic characterization of airlift tower loop bioreactors with and without motionless mixtures. *Bioprocess Engineering*, 12, 119–130.
- Sakai, N., Onozaki, M., Saegusa, H., Ishibashi, H., Hayashi, T., Kobayashi, M., Tachikawa, N., Ishikawa, I., & Morooka, S. (2000). Fluid dynamics in coal liquefaction reactors using neutron absorption tracer technique. *American Institute of Chemical Engineers Journal*, 46, 1688–1693.
- Salesse, A., Larue de Tournemine, A., & Roig, V. (2001). Development of bubble cluster detection and identification method. *Fifth World conference on experimental heat transfer, fluid mechanics and thermodynamics*, Thessaloniki, Greece, September 24–28, 2001.
- Samways, A. L., & Bruun, H. H. (1992). *Vertical up-flow of oil/water mixtures*. Technical Report No. 200, Department of Mechanical and Manufacturing Engineering, University of Bradford, UK.
- Saroha, A. K., & Nigam, K. D. P. (1996). Trickle bed reactors. *Reviews in Chemical Engineering*, 12, 207–347.
- Schmitz, D., & Mewes, D. (2000). Tomographic imaging of transient multiphase flow in bubble columns. *Chemical Engineering Journal*, 77, 99–104.
- Schügerl, K. (1982). Characterization and performance of single and multistage tower reactors with outer loop for cell mass production. *Advances in Biochemical Engineering*, 22(93), 93–117.
- Schweitzer, J. M., Bayle, J., & Gauthier, T. (2001). Local gas hold-up measurements in fluidized bed and slurry bubble column. *Chemical Engineering Science*, 56, 1103–1110.
- Sederman, A. J., Johns, M. L., Alexander, P., & Gladden, L. F. (1998). Structure–flow correlations in packed beds. *Chemical Engineering Science*, 53, 2117–2128.
- Sederman, A. J., Johns, M. L., Bramley, A. S., Alexander, P., & Gladden, L. F. (1997). Magnetic resonance imaging of liquid flow and pore structure within packed beds. *Chemical Engineering Science*, 52, 2239–2250.
- Serizawa, A., Kataoka, I., & Mishigoshi, I. (1975). Turbulence structure of air–water bubbly flow. *International Journal of Multiphase Flow*, 2, 221–259.
- Shah, Y. T., Stiegel, G. J., & Sharma, M. M. (1978). Backmixing in gas–liquid reactors. *American Institute of Chemical Engineers Journal*, 24, 369–400.
- Sharma, S., Mantle, M. D., Gladden, L. F., & Winterbottom, J. M. (2001). Determination of bed voidage using water substitution and 3D magnetic resonance imaging, bed density and pressure drop in packed-bed reactors. *Chemical Engineering Science*, 56, 587–593.
- Shen, G., & Finch, J. A. (1996). Bubble swarm velocity in a column. *Chemical Engineering Science*, 51, 3665–3674.
- Shepp, L. A., & Logan, B. F. (1974). The Fourier reconstruction of a head section. *IEEE Transactions on Nuclear Science*, NS-21, 21–43.
- Smith, G. B., Gamblin, B. R., & Newton, D. (1995). X-ray imaging of slurry bubble column reactors: The effects of systems pressure and scale. *Transactions of the Institution of Chemical Engineers, A: Chemical Engineering Research and Design*, 73, 632–636.
- Souhar, M. (1982). *Contribution à l'étude dynamique des écoulements diphasiques gaz–liquide en conduite verticale: cas des régimes à bulles et à poches*. Thèse de doctorat d'état, Institut National Polytechnique de Lorraine, Nancy, France.
- Souhar, M. (1987). Etude expérimentale de la turbulence près de la paroi en écoulement à bulles. *International Journal of Heat Mass Transfer*, 30, 1813–1823.
- Storck, A., Latifi, M. A., Barthole, G., Laurent, A., & Charpentier, J. C. (1986). Electrochemical study of liquid–solid mass transfer in packed bed electrodes with upward and downward cocurrent gas–liquid flow. *Journal of Applied Electrochemistry*, 16, 947–963.
- Stravs, A. A., & von Stockar, U. (1985). Measurement of interfacial areas in gas–liquid dispersions by ultrasonic pulse transmission. *Chemical Engineering Science*, 40, 1169–1175.
- Stravs, A. A., Wahl, J., von Stockar, U., & Reilly, P. J. (1987). Development of an ultrasonic pulse reflection method for measuring relative size distributions of air bubbles in aqueous solutions. *Chemical Engineering Science*, 42, 1677–1987.
- Svendsen, H. F., Luo, H. A., Hjarbo, K. W., & Jakobsen, H. A. (1998). Experimental determination and modelling of bubble-size distributions in bubble columns. *Chinese Journal of Chemical Engineering*, 6(1), 29–41.
- Thang, N. T., & Davis, M. R. (1979). The structure of bubbly flow through Venturis. *International Journal of Multiphase Flow*, 5, 17–37.
- Thimmapuram, P. R., Rao, N. S., & Saxena, S. C. (1992). Characterization of hydrodynamic regimes in a bubble column. *Chemical Engineering Science*, 47, 3355–3362.
- Toral, H. (1981). A study of the hot-wire anemometer for measuring void fraction in two-phase flow. *Journal of Physics E: Science and Instruments*, 14, 822–827.
- Toye, D. (1996). *Etude de l'écoulement ruisselant dans les lits fixes par tomographie à rayons X*. Thèse de Doctorat en Sciences Appliquées, Université de Liège, Belgium.
- Uga, T. (1972). Determination of bubble-size distribution in a BWR. *Nuclear Engineering and Design*, 22, 252–261.
- Uribe-Salas, A., Gomez, C. O., & Finch, J. A. (1994). A conductivity technique for gas and solids holdup determination in three-phase reactors. *Chemical Engineering Science*, 49, 1–10.
- Utiger, M., Stüber, F., Duquenne, A. M., Delmas, H., & Guy, C. (1999). Local measurements for the study of external loop airlift hydrodynamics. *Canadian Journal of Chemical Engineering*, 77, 375–382.
- Vial, C. (2000). *Apport de la mécanique des fluides à l'étude des contacteurs gaz/liquide: Expérience et simulation numérique*. Thèse de doctorat, Institut National Polytechnique de Lorraine, Nancy, France.
- Vial, C., Camarasa, E., Poncin, S., Wild, G., Midoux, N., & Bouillard, J. (2000). Study of hydrodynamic behaviour in bubble columns and external loop airlift reactors through analysis of pressure fluctuations. *Chemical Engineering Science*, 55, 2957–2973.
- Vial, C., Lainé, R., Poncin, S., Midoux, N., & Wild, G. (2001a). Influence of gas distribution and regime transition on liquid velocity and turbulence in a 3-D bubble column. *Chemical Engineering Science*, 56, 1085–1093.
- Vial, C., Poncin, S., Wild, G., & Midoux, N. (2001b). A simple method for regime identification and flow characterisation in bubble columns and airlift reactors. *Chemical Engineering and Processing*, 40, 35–151.
- Villermaux, J. (1995). *Génie de la Réaction Chimique* (2nd ed.). Technique et Documentation, Lavoisier, Paris.
- Villermaux, J., & van Swaaij, W. P. M. (1969). Modèle représentatif de la distribution des temps de séjour dans un réacteur semi-infini à dispersion axiale avec zones stagnantes. Application à l'écoulement ruisselant dans des colonnes d'anneaux Raschig. *Chemical Engineering Science*, 24, 1097–1111.
- Wallis, G. B. (1969). *One-dimensional two-phase flow*. New York: McGraw-Hill.
- Wang, S. K., Lee, S. J., Jones, O. C., & Lahey, R. T. (1990). Statistical analysis of turbulent two-phase pipe flow. *American Society of Mechanical Engineers—Journal of Fluids Engineering*, 112, 89–95.

- Warsito, M., Ohkawa, N., Kawata, S., & Uchida, S. (1999). Cross-sectional distributions of gas and solid holdups in slurry bubble column investigated by ultrasonic computed tomography. *Chemical Engineering Science*, *54*(21), 4711–4728.
- Wild, G., & Poncin, S. (1996). Hydrodynamics of three-phase sparged reactors. In K.D.P. Nigam, & A. Schumpe (Eds.), *Three-phase sparged reactors* (pp. 11–113). New York: Gordon and Breach Science Publishers, Topics in Chemical Engineering Series.
- Wolff, C. (1989). *Untersuchungen mit Mehrkanal-Mikrosonden zum Einfluß suspendierter Feststoffe auf die Hydrodynamik in Blasensäulen-Reaktoren für Chemie und Biotechnologie* VDI-Fortschrittsberichte Reihe 3 (Verfahrenstechnik) Nr 176. Düsseldorf, (Germany): VDI-Verlag.
- Wolff, C., Briegleb, F. U., Bader, J., Hektor, K., & Hammer, H. (1990). Measurements with multi-point micropobes. *Chemical Engineering Technology*, *13*, 172–184.
- Yang, X. L., Euzen, J. P., & Wild, G. (1990). Residence time distribution of the liquid in gas–liquid cocurrent upflow fixed bed reactors with porous particles. *Chemical Engineering Science*, *45*, 3311–3317.
- Yao, B. P., Zheng, C., Gasche, H. E., & Hofmann, H. (1991). Bubble behaviour and flow structure of bubble columns. *Chemical Engineering and Processing*, *29*, 65–75.
- Young, M. A., Carbonell, R. G., & Ollis, D. F. (1991). Airlift bioreactors: Analysis of local two-phase hydrodynamics. *American Institute of Chemical Engineers Journal*, *37*, 403–428.
- Yu, Y. H., & Kim, S. D. (1991). Bubble properties and local liquid velocity in the radial direction of cocurrent gas–liquid flow. *Chemical Engineering Science*, *46*, 313–320.
- Zahradník, J., Fialová, M., Ruzicka, M., Drahos, J., Kastanek, F., & Thomas, N. H. (1997). Duality of the gas–liquid flow regimes in bubble column reactors. *Chemical Engineering Science*, *52*, 3811–3826.
- Züber, N., & Findlay, J. A. (1965). Average volumetric concentration in two-phase flow systems. *Journal of Heat Transfer*, *87*, 453–468.